SUPPLEMENTARY MATERIAL

Testing the limitations of harmonic approximation in the determination of Raman intensities

Ankit Raj* and Yen-Bang Chao
Department of Applied Chemistry and Institute of Molecular Science, National Yang Ming Chiao Tung University, Hsinchu 30010, Taiwan

Henryk A. Witek†
Department of Applied Chemistry and Institute of Molecular Science, National Yang Ming Chiao Tung University, Hsinchu 30010, Taiwan and Center for Emergent Functional Matter Science, National Yang Ming Chiao Tung University, Hsinchu 30010, Taiwan

---

Contents

---

* ankit@nycu.edu.tw
† hwitek@nycu.edu.tw

List of Tables

List of Figures

List of symbols

γ	: polarizability anisotropy, $\gamma = \alpha_{\parallel} - \alpha_{\perp}$	[a.u. or other specified unit]
$\bar{\alpha}$	: mean polarizability , $\bar{\alpha} = (2\alpha_{\perp} + \alpha_{\parallel})/3$	[a.u. or other specified unit]
λ	: Wavelength	[nm]
$\psi_{v,J}$	: Wavefunction corresponding to specific vibrational state (v) and state (v) and rotational state (J) in the ground electronic state	
Ω	: Operator	

S1. Selection rules for harmonic oscillator

The time-independent Schrödinger equation for harmonic oscillator is given by

$$\frac{1}{2m}\left(-\hbar\frac{d^2\phi(x)}{dx^2}+\mu^2\omega^2x^2\phi(x)\right)=E\phi(x) \tag{E1}$$

where the wave function $\phi(x)$ is expressed using the Hermite polynomials $H_n(\xi)$ as

$$\phi_n(x)=(\frac{\alpha}{\pi})^{1/4}\frac{1}{\sqrt{2^n n!}}H_n(\xi)e^{\frac{-\xi^2}{2}} \tag{E2}$$

where

$$\alpha=\frac{\mu\omega}{\hbar}\text{ and }\xi=\sqrt{\alpha}x\,. \tag{E3}$$

The Hermite polynomials $H_n(\xi)$ for $n=0-3$ are listed below:

$$\begin{aligned}H_0(\xi)&=1\\H_1(\xi)&=2\xi\\H_2(\xi)&=4\xi^2-2\\H_3(\xi)&=8\xi^3-12\xi.\end{aligned} \tag{E4}$$

This set of Hermite polynomials in Eqn. E2 satisfies the properties of the harmonic wave functions. They are even-function when the value of n in Eqn. E2 is even, while they are are odd for odd n.

Ladder operators are introduced to derive the selection rules of harmonic oscillator. In Eqn. E5, a_+ is the raising operator, while a_- is the lowering operator.

$$\begin{aligned}a_+=&\frac{1}{\sqrt{2\hbar\mu\omega}}(-ip+\mu\omega x)\\a_-=&\frac{1}{\sqrt{2\hbar\mu\omega}}(ip+\mu\omega x)\end{aligned} \tag{E5}$$

These operators can then be used to construct wave functions corresponding to higher and lower vibrational state with respect to certain initial state (e.g. for a given vibrational state defined by index n, we can obtain the wave functions for the higher and lower vibrational states by the operation of the a_+ and a_- operators, respectively.)

Suppose ϕ_n is the normalized the wave function for a given vibrational state, satisfying the condition, $\int_{-\infty}^{\infty}\phi_n^2dx=1$ for all of $n=0,1,...\infty$. Our goal then is to find the constant c_+ and c_- accompanying the ladder operators which fulfill the following conditions:

$$\begin{aligned}\phi_{n+1}=&c_+a_+\phi_n\\\phi_{n-1}=&c_-a_-\phi_n.\end{aligned} \tag{E6}$$

For example, taking the norm of the raised state obtained from the a_+ operator and using the property of Hermitian conjugates for a_+ and a_- we obtain

$$\begin{aligned}\int_{-\infty}^{\infty}\phi_n^2dx=&c_+^2\int_{-\infty}^{\infty}(a_+\phi_n(x))^*(a_+\phi_n(x))dx\\=&c_+^2\int_{-\infty}^{\infty}(a_-a_+\phi_n(x))^*(\phi_n(x))dx\end{aligned} \tag{E7}$$

where the operator a_-a_+ is related to the as Hamiltonian, $H=\hbar\omega(a_-a_++\frac{1}{2})$. Therefore,

$$a_-a_+\phi_n=(\frac{H}{\hbar\omega}+\frac{1}{2})\phi_n=(\frac{1}{2}+n+\frac{1}{2})\phi_n. \tag{E8}$$

Substitution of equation (E8) into the integral (E7) gives

$$c_+^2\int_{-\infty}^{\infty}(a_-a_+\phi_n(x))^*(\phi_n(x))dx=c_+^2(n+1)\int_{-\infty}^{\infty}\phi_n^2dx=1, \tag{E9}$$

and results in the normalization constant, $c_+ = \frac{1}{\sqrt{n+1}}$ for raising operator a_+. Similarly, $c_- = \frac{1}{\sqrt{n}}$ can be derived using the same procedure.

The final expressions for the operation of ladder operators on the Harmonic wave functions are

$$\begin{aligned} \phi_{n+1} &= \frac{1}{\sqrt{n+1}} a_+ \phi_n \\ \phi_{n-1} &= \frac{1}{\sqrt{n}} a_- \phi_n. \end{aligned} \tag{E10}$$

A. Orthonormality

The harmonic wave functions ϕ_n must be orthonormal. Taking integral for two such wavefunctions denoted as ϕ_n and ϕ_m, where $n, m = 0, 1, ...\infty$, we obtain

$$\langle \phi_n(x) | \phi_m(x) \rangle = \frac{1}{\sqrt{m!}} \frac{1}{\sqrt{n!}} \int_{-\infty}^{\infty} (a_+^n \phi_0)^* (a_+^m \phi_0) dx. \tag{E11}$$

We suppose that $m > n$, and the a_+ and a_- operators are Hermitian conjugate. These properties are used to simplify $a_+^n \phi_0$ to ϕ_n in Eqn. E12.

$$\frac{1}{\sqrt{m!}} \frac{1}{\sqrt{n!}} \int_{-\infty}^{\infty} (a_+^n \phi_0)^* (a_+^m \phi_0) dx = \frac{1}{\sqrt{m!}} \frac{1}{\sqrt{n!}} \int_{-\infty}^{\infty} (a_-^m a_+^n \phi_0)^* (\phi_0) dx \tag{E12}$$

Next, the obtained term, $a_-^m \phi_n$ is evaluated to ϕ_{n-m}. However, since the condition of $m > n$ is imposed, ϕ_{n-m} results to 0.

Similarly, in another case where we assume that $n > m$ while the raising and lowering operators are Hermitian conjugates. In the same way $a_+^m \phi_0$ is simplified to ϕ_m, and $a_-^n \phi_m$ to ϕ_{m-n}, in Eqn. E13.

$$\frac{1}{\sqrt{m!}} \frac{1}{\sqrt{n!}} \int_{-\infty}^{\infty} (a_+^n \phi_0)^* (a_+^m \phi_0) dx = \frac{1}{\sqrt{m!}} \frac{1}{\sqrt{n!}} \int_{-\infty}^{\infty} (\phi_0)^* (a_-^n a_+^m \phi_0) dx \tag{E13}$$

Again, since the condition of $n > m$ is imposed, ϕ_{m-n} results to 0.

Hence, only when $m = n$, the integral in Eqn. E11 is nonzero. Since, ϕ_n is the normalizes wave function, satisfying $\int \phi_n^2 dx = 1$, hence, orthogonality of the harmonic wave functions is summarized as

$$\langle \phi_m(x) | \phi_n(x_k) \rangle = \begin{Bmatrix} 0 & \text{for} & m \neq n \\ 1 & \text{for} & m = n \end{Bmatrix}. \tag{E14}$$

B. Expectation values

Rearranging the Eqn. E5, we can find the operator x in terms of a_+ and a_- as

$$x = \sqrt{\frac{\hbar}{2\mu\omega}} (a_+ + a_-). \tag{E15}$$

Next, the expectation value of x for a transition from the m^{th} vibrational state to n^{th} vibrational state is given by

$$\langle x \rangle = \langle \phi_m(x) | x | \phi_n(x) \rangle = \sqrt{\frac{\hbar}{2\mu\omega}} \int_{-\infty}^{\infty} \phi_m(x)^* (a_+ + a_-) \phi_n(x) dx \, . \tag{E16}$$

This integral can be separated into two terms: the first is related to the raising operator a_+, while the other is related to lowering operator a_-.

$$\sqrt{\frac{\hbar}{2\mu\omega}} \int_{-\infty}^{\infty} \phi_m(x)^* (a_+ + a_-) \phi_n(x) dx = \sqrt{\frac{\hbar}{2\mu\omega}} \int_{-\infty}^{\infty} \phi_m(x)^* a_+ \phi_n(x) dx + \sqrt{\frac{\hbar}{2\mu\omega}} \int_{-\infty}^{\infty} \phi_m(x)^* a_- \phi_n(x) dx \tag{E17}$$

where $a_+\phi_n(x) = \sqrt{n+1}\phi_{n+1}(x)$ in the first term results in

$$\sqrt{\frac{\hbar}{2\mu\omega}}\int_{-\infty}^{\infty}\phi_m(x)^* a_+\phi_n(x)dx = \sqrt{n+1}\sqrt{\frac{\hbar}{2\mu\omega}}\int_{-\infty}^{\infty}\phi_m(x)^*\phi_{n+1}(x)dx, \tag{E18}$$

and similarly $a_-\phi_n(x) = \sqrt{n}\phi_{n-1}(x)$ in the second term gives

$$\sqrt{\frac{\hbar}{2\mu\omega}}\int_{-\infty}^{\infty}\phi_m(x)^* a_-\phi_n(x)dx = \sqrt{n}\sqrt{\frac{\hbar}{2\mu\omega}}\int_{-\infty}^{\infty}\phi_m(x)^*\phi_{n-1}(x)dx. \tag{E19}$$

From the property of orthogonality, the integral $\int_{-\infty}^{\infty}\phi_m(x)^*\phi_{n+1}(x)dx$ in Eqn. E18 is unity only when $m = n+1$. Similarly, the integral $\int_{-\infty}^{\infty}\phi_m(x)^*\phi_{n-1}(x)dx$ in Eqn. E19 is unity only when $m = n-1$. The expectation values are then obtained as

$$\langle\phi_m(x)|x|\phi_n(x)\rangle = \left\{\begin{array}{cc} 0 & \text{for otherwise} \\ \sqrt{n+1}b & \text{for } m = n+1 \\ \sqrt{n}b & \text{for } m = n-1 \end{array}\right\} \tag{E20}$$

where

$$b = \sqrt{\frac{\hbar}{2\mu\omega}} \tag{E21}$$

for the harmonic oscillator. Thus, the results on the orthogonality and expectation values for harmonic oscillator allow only transitions of the type $\Delta v = \pm 1$.

S2. Design of bond function

In our earlier work, we have performed calculations for the polarizabilities and their matrix elements for molecular hydrogen.[45] We found that the computed polarizabilities for H_2 show considerable improvement in the accuracy with the introduction of bond-functions (BF). Further, the computed values approached the accuracy of results computed using explicitly correlated wave functions reported by Rychlewski.[46] With this motivation in mind, we aim at developing analogous bond-functions for other diatomic molecules. We start this procedure by first analyzing the change in energy of the molecule with the introduction of various types of the bond-functions (such as s, p, d, f, and g functions) with a range of exponents. Next, we study the change in the energy of the molecule while placing the bond-functions at various locations across the bond axis.

1. *Analysis of the computed energies of the studied molecules with the inclusion of various bond-functions*

In these tests, the energy of the molecule was computed, first, without any bond-function basis. Next, various bond-functions with angular momentum L =0–4 (s, p, d, f, and g) were introduced at mid-bond position. The energy computations were performed with different exponents of the primitive functions. In general, all the molecules showed a lowering in the energy with the introduction of a bond-function (see Fig. F1–F13). Functions with larger L, such as f, and the g functions, led to a prominent decrease in the energy of the molecule.

The results obtained for the HF molecule with different bond-functions are shown in Fig. F1. The $f-$function was chosen as the largest function type, and whose exponents were determined by scanning the molecular energies over different exponents. This is shown in Fig. F2. (In all such figures showing the scans of exponents, the darker regions represent lower energy.) The even-tempered functions were generated using the expression $\alpha\beta^{1-k}$, where α is the leading exponent, and β represents the ratio between the subsequent exponents.

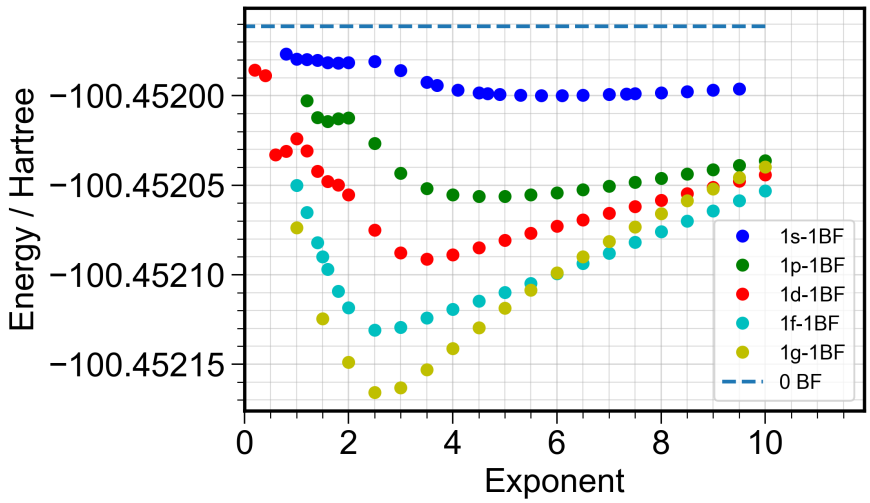

FIG. F1: CCSD(T) energy of the HF molecule without any bond-functions (dashed line), and with bond-functions (colored circles) with different exponents. The energies were computed at r=0.91695 Å (1.73278 Bohr). Introduction of any type of bond-function results in a lowering of the energy, with the larger functions showing more prominent decrease.

A similar procedure was followed for the $4d-$ and $5p-$ functions for which the individual scans are shown in Fig. F3 and Fig. F4, respectively.

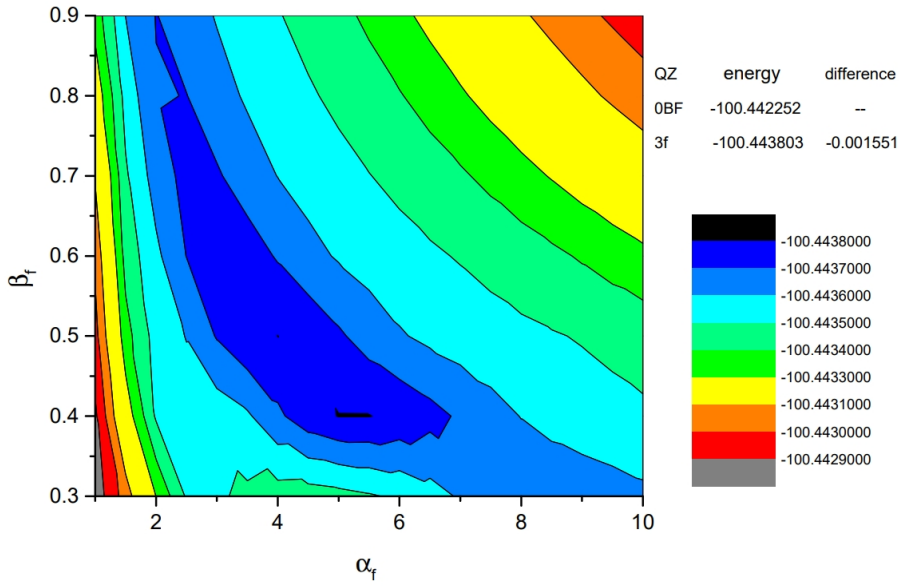

FIG. F2: Analysis of the molecular energies of HF computed using CCSD(T) methodology over the exponents of the introduced *f*-type bond-functions. The AO basis was *aug-cc-pVQZ* for the H-atom and *aug-cc-pwCVQZ* for the F atom. In this 2-D plot, the dark blue to black regions represent lower energy.

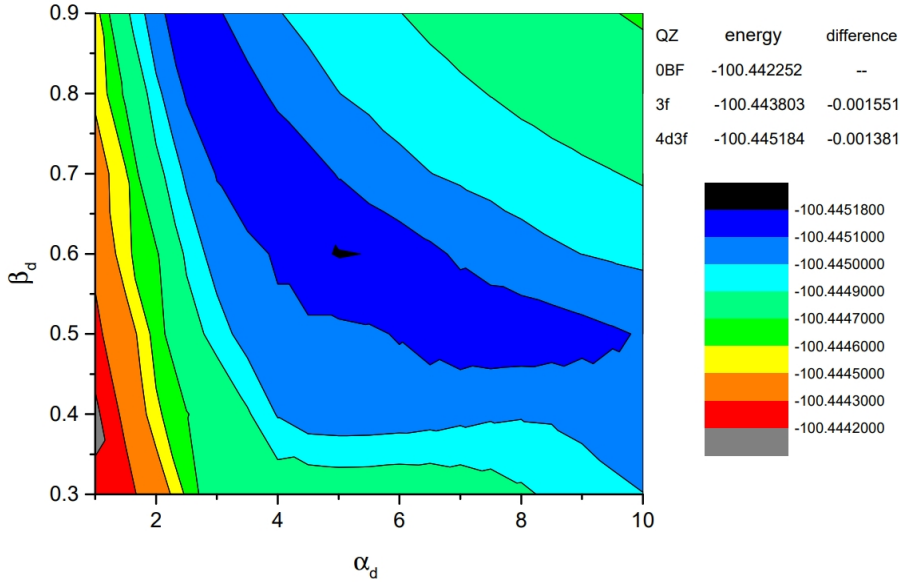

FIG. F3: Analysis of the molecular energies of HF computed using CCSD(T) methodology over the exponents of the introduced *d*-type bond-functions. The AO basis was *aug-cc-pVQZ* for the H-atom and *aug-cc-pwCVQZ* for the F atom.

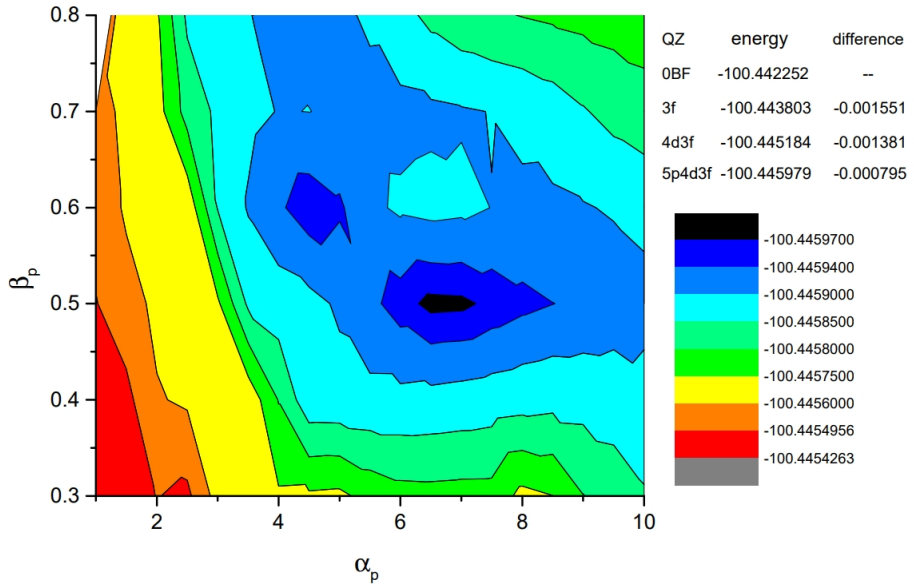

FIG. F4: Analysis of the molecular energies of HF computed using CCSD(T) methodology over the exponents of the introduced *p*-type bond-functions. The AO basis was *aug-cc-pVQZ* for the H-atom and *aug-cc-pwCVQZ* for the F atom.

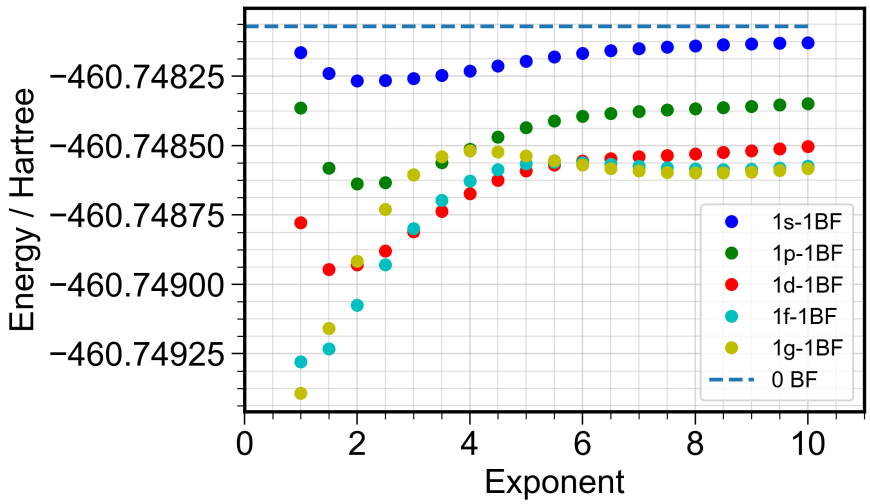

FIG. F5: CCSD(T) energy of the HCl molecule without any bond-functions (dashed line), and with bond-functions (colored circles) with different exponents. The energies were computed at r=1.27 Å (2.39995 Bohr). Introduction of any function results in lowering of the energy with the larger functions showing a prominent decrease.

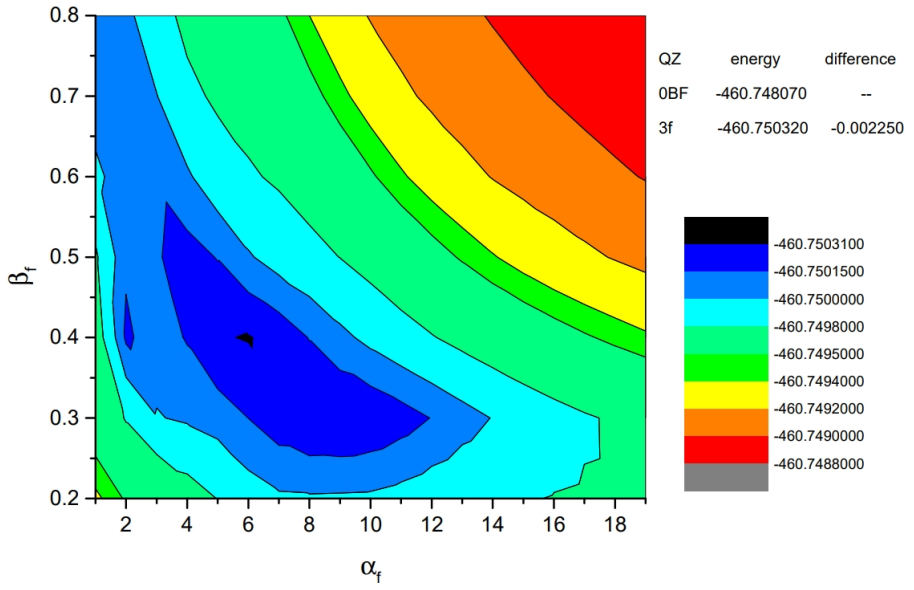

FIG. F6: Analysis of the molecular energies of HCl computed using CCSD(T) methodology over the exponents of the introduced *f*-type bond-functions. The AO basis was *aug-cc-VQZ* for the H atom and *aug-cc-pwCVQZ* for the Cl atom.

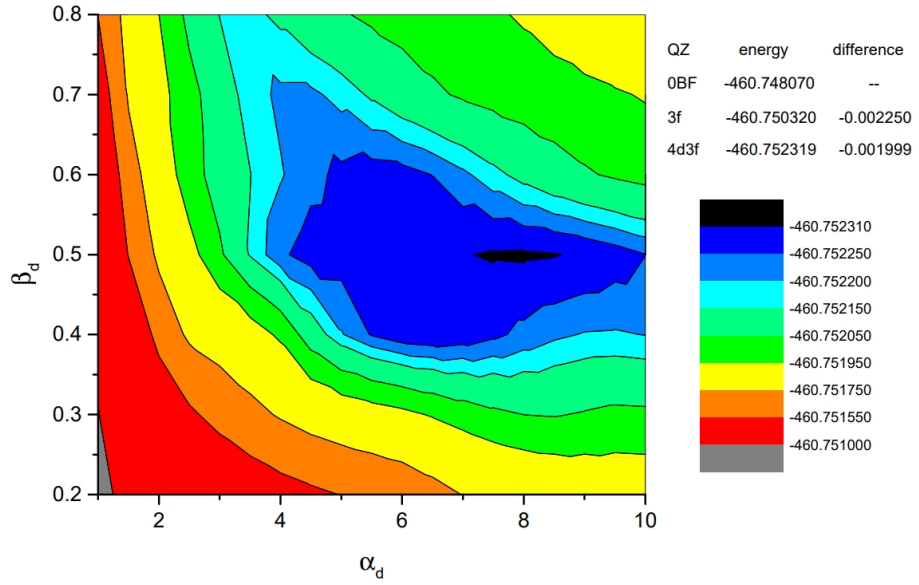

FIG. F7: Analysis of the molecular energies of HCl computed using CCSD(T) methodology over the exponents of the introduced *d*-type bond-functions. The AO basis was *aug-cc-VQZ* for the H atom and *aug-cc-pwCVQZ* for the Cl atom.

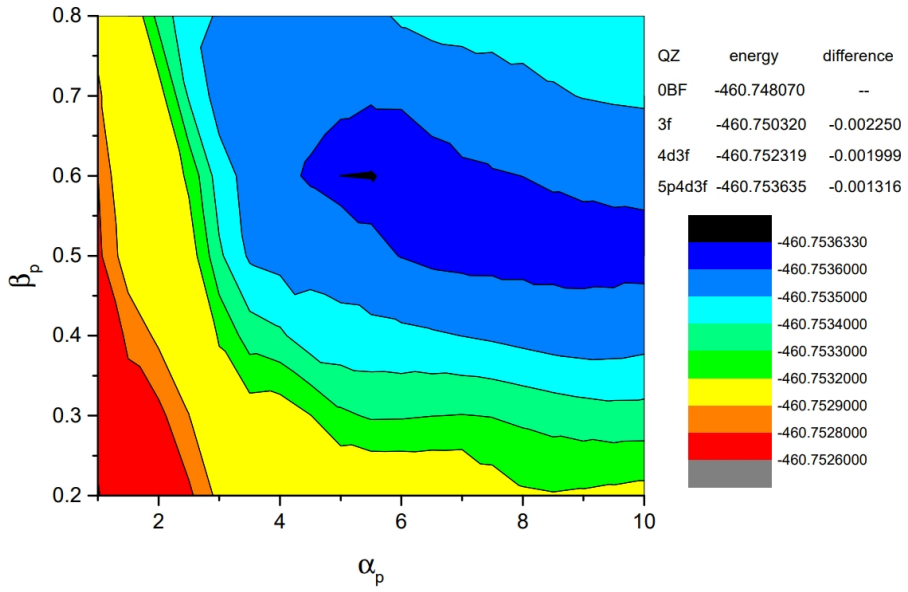

FIG. F8: Analysis of the molecular energies of HCl computed using CCSD(T) methodology over the exponents of the introduced *p*-type bond-functions. The AO basis was *aug-cc-VQZ* for the H atom and *aug-cc-pwCVQZ* for the Cl atom.

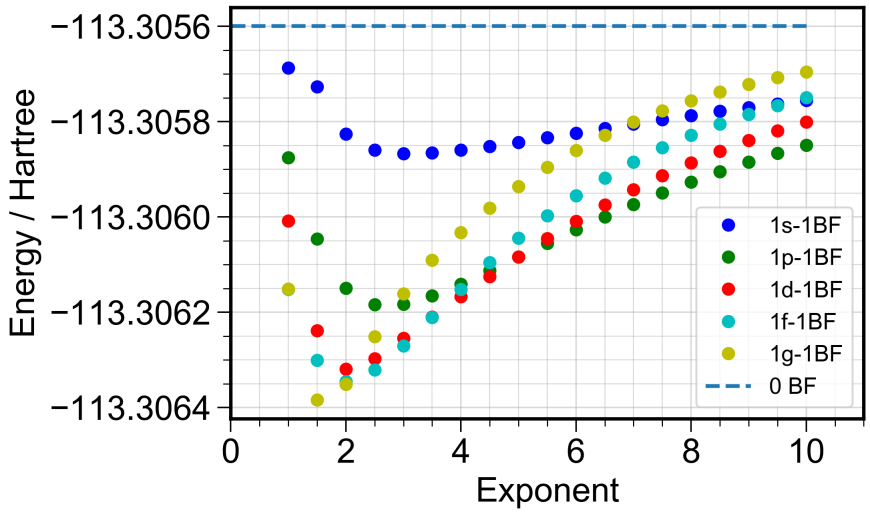

FIG. F9: CCSD(T) energy of the CO molecule without any bond-functions (dashed line), and with bond-functions (colored circles) with different exponents. The energies were computed at *r*=1.12783 Å (2.13128 Bohr). Introduction of any function results in lowering of the energy with the larger functions showing a prominent decrease.

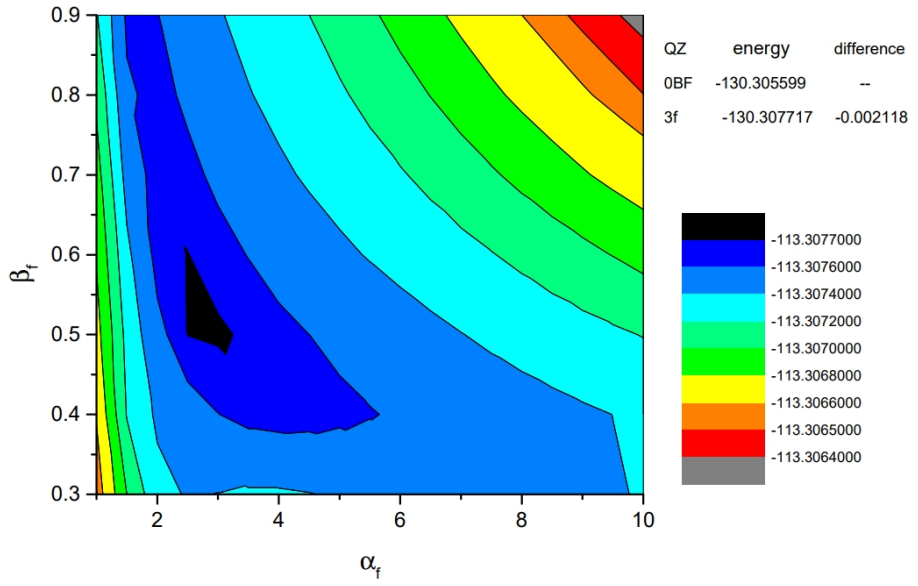

FIG. F10: Analysis of the molecular energies of CO computed using CCSD(T) methodology over the exponents of the introduced *f*-type bond-functions. The AO basis was *aug-cc-pwCVQZ* for the C and O atom.

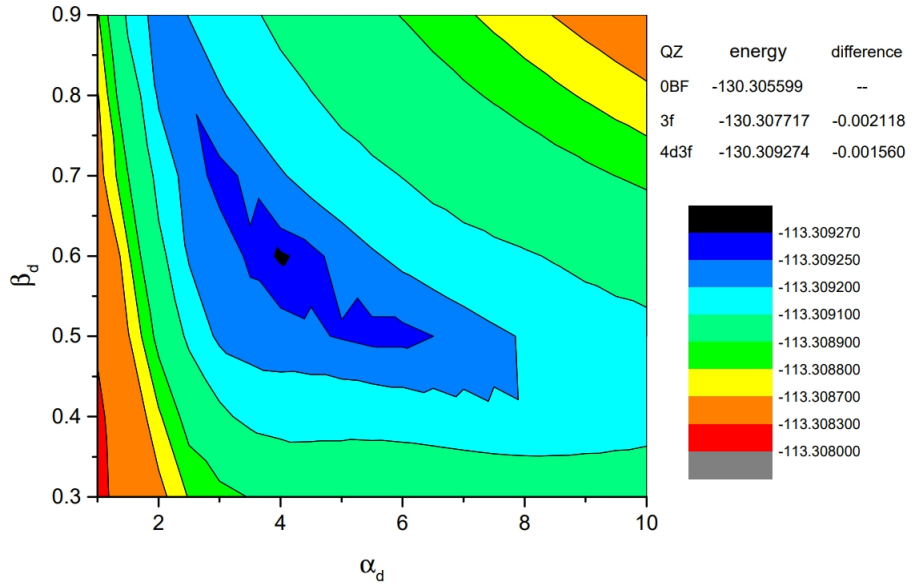

FIG. F11: Analysis of the molecular energies of CO computed using CCSD(T) methodology over the exponents of the introduced *d*-type bond-functions. The AO basis was *aug-cc-pwCVQZ* for the C and O atom.

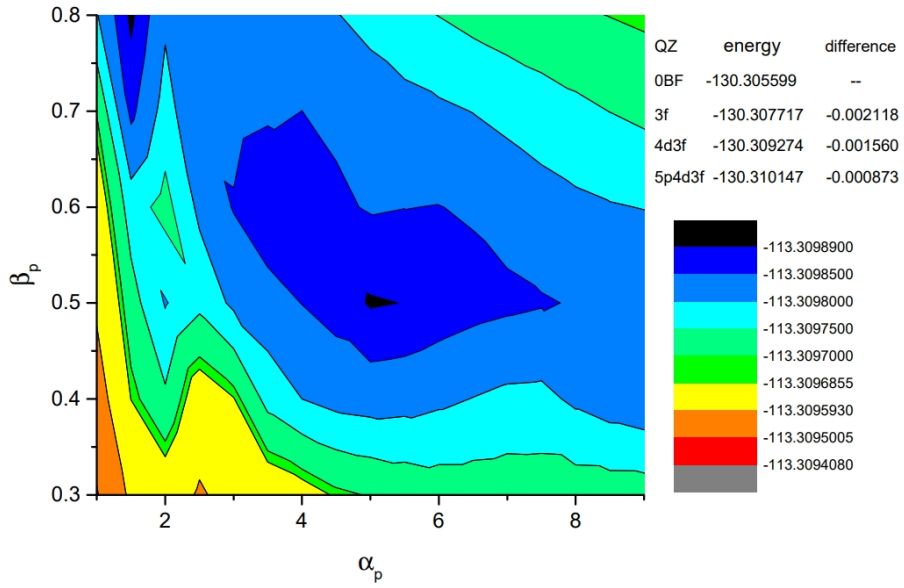

FIG. F12: Analysis of the molecular energies of CO computed using CCSD(T) methodology over the exponents of the introduced *p*-type bond-functions. The AO basis was *aug-cc-pwCVQZ* for the C and O atom.

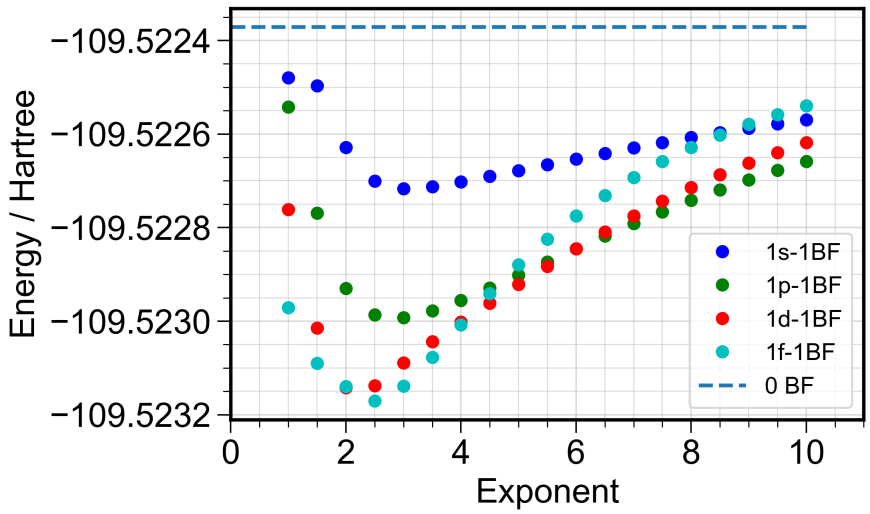

FIG. F13: CCSD(T) energy of the N_2 molecule without any bond-functions (dashed line), and with bond-functions (colored circles) with different exponents. The energies were computed at r=1.09434 Å (2.06800 Bohr). Introduction of any function results in lowering of the energy with the larger functions showing a prominent decrease.

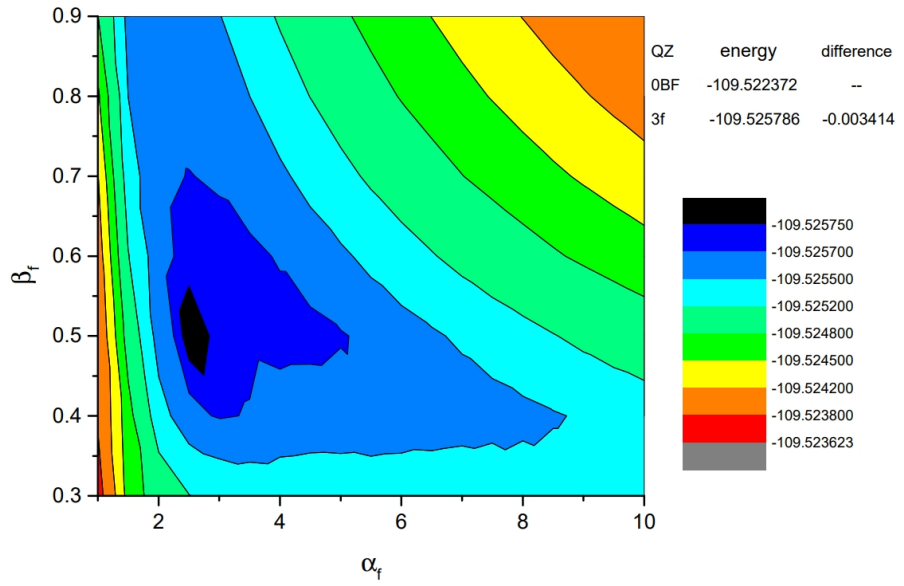

FIG. F14: Analysis of the molecular energies of N_2 computed using CCSD(T) methodology over the exponents of the introduced *f*-type bond-functions. The AO basis was *aug-cc-pwCVQZ* for the N atom.

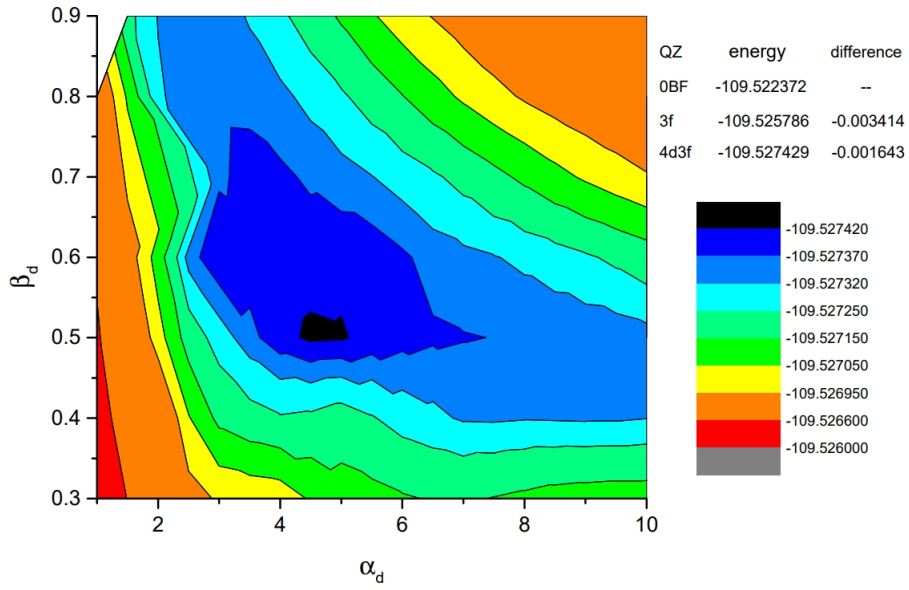

FIG. F15: Analysis of the molecular energies of N_2 computed using CCSD(T) methodology over the exponents of the introduced *d*-type bond-functions. The AO basis was *aug-cc-pwCVQZ* for the N atom.

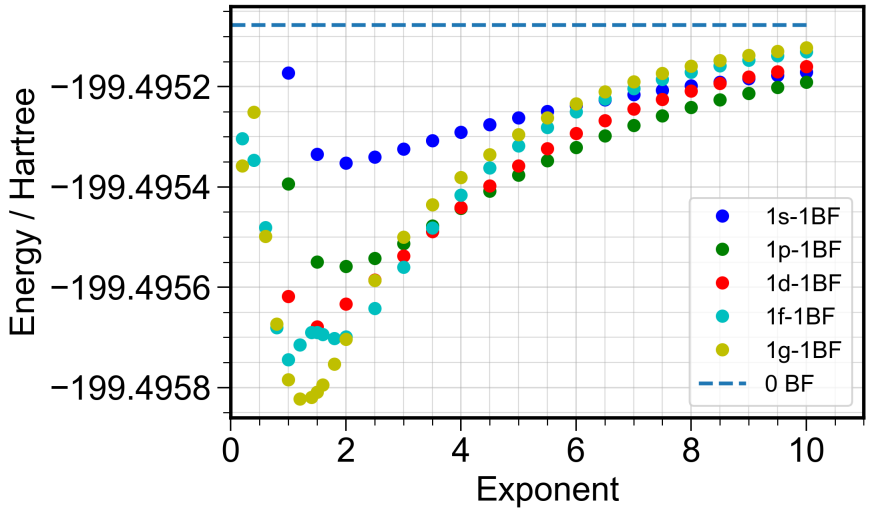

FIG. F16: CCSD(T) energy of the F_2 molecule without any bond-functions (dashed line), and with bond-functions (colored circles) with different exponents. The energies were computed at r=1.41193 Å (2.66816 Bohr). Introduction of any function results in lowering of the energy with the larger functions showing a prominent decrease.

2. *Analysis of the computed energies of the studied molecules with the bond-functions located at different positions*

In the following section, results on the CCSD(T) energies of the molecule with bond-function included at different positions along the inter-nuclear distance are presented. The distance between the more electronegative atom (in the studied molecule) and the bond-function is used as the x-axis, while the corresponding energy is plotted as the y-axis.

Fig. F20 shows the energy of the CO molecule as the position of the bond-function is changed. The AO basis used in this case is *aug-cc-pwCVQZ* (from the EMSL database[47]) while the bond-function is even-tempered $4d3f$ function (constructed as $\alpha\beta^k$, where α =3.5, β =0.5 for the $d-$function, and α =3.0, β =0.5 for the $f-$function).

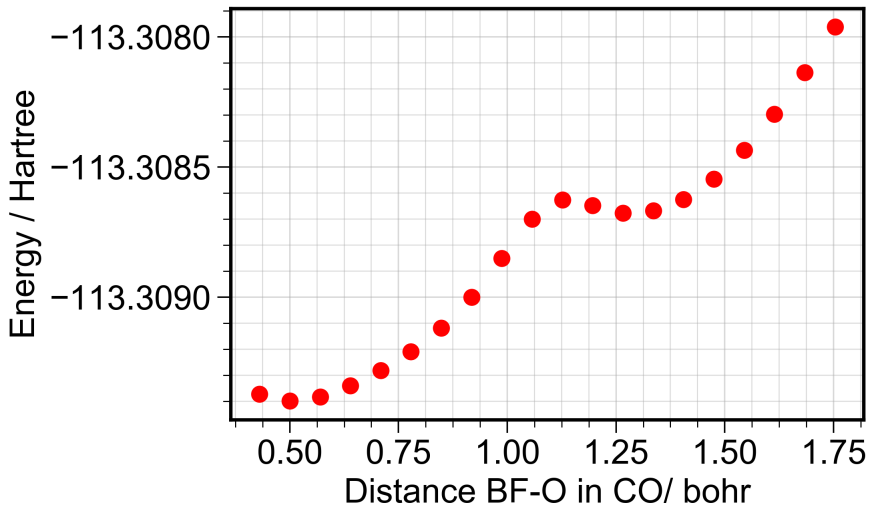

FIG. F20: CCSD(T) energy of the CO molecule with the introduction of bond-functions at different locations along the inter-nuclear distance. Distance of 0.75589 Bohr from the O-atom was chosen for placing the bond-functions in the final computations.

Fig. F21 shows the energy of the HCl molecule as the position of the bond-function is changed. The AO

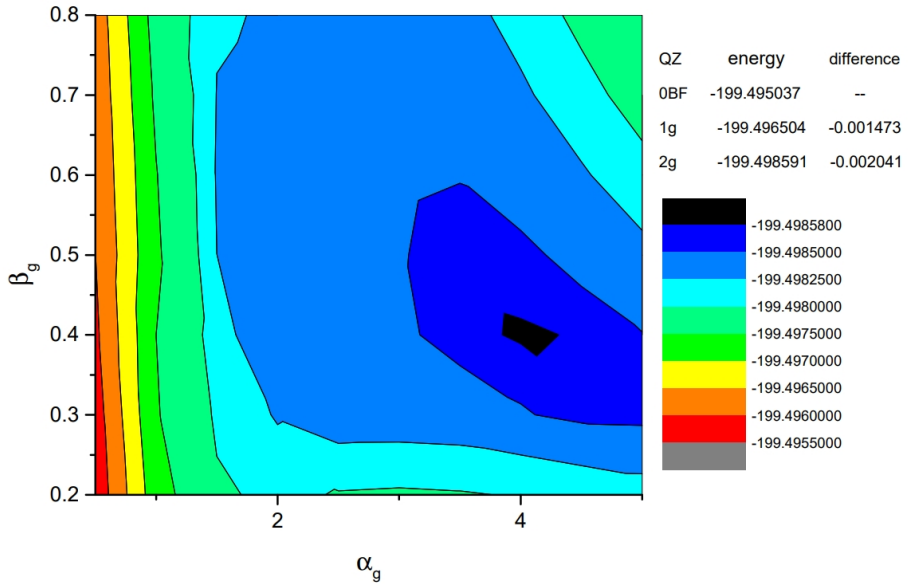

FIG. F17: Analysis of the molecular energies of F_2 computed using CCSD(T) methodology over the exponents of the introduced *g*-type bond-functions. The AO basis was *aug-cc-pwCVQZ* for the F atom.

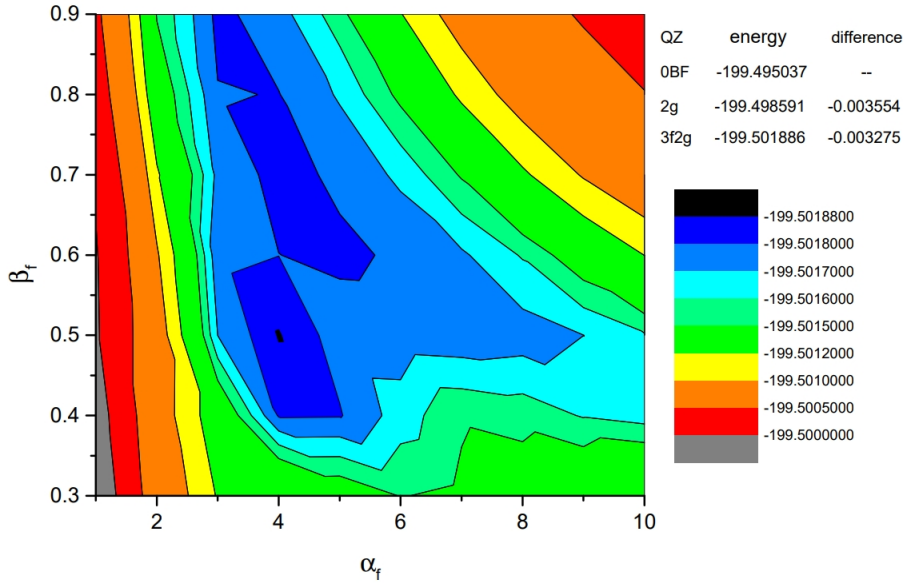

FIG. F18: Analysis of the molecular energies of F_2 computed using CCSD(T) methodology over the exponents of the introduced *f*-type bond-functions. The AO basis was *aug-cc-pwCVQZ* for the F atom.

basis used in this case is *aug-cc-pVQZ* for the H-atom and *aug-cc-pwCVQZ* for the Cl atom (from the EMSL database[47]). The bond-function is even-tempered $1f$ function (constructed as $\alpha\beta^k$, where α =1.5, β =1 for the $f-$function).

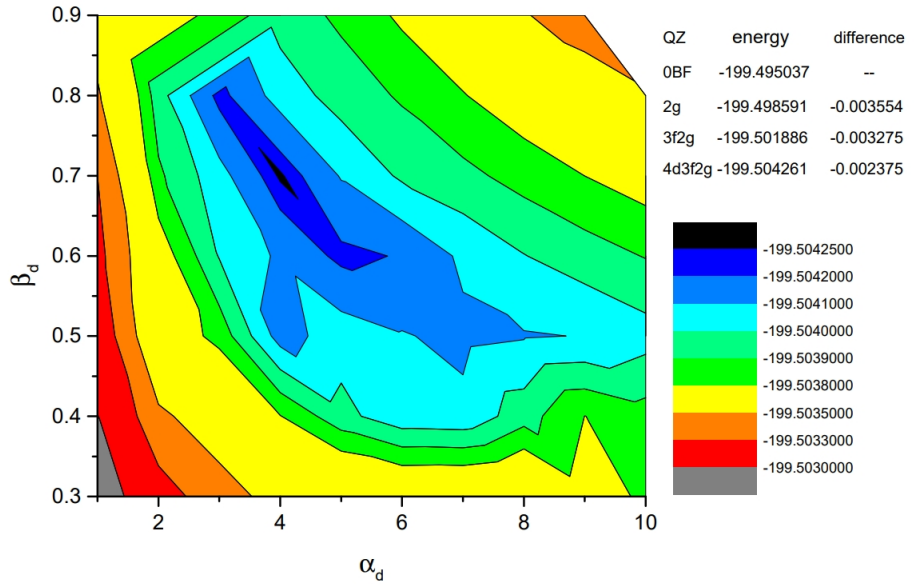

FIG. F19: Analysis of the molecular energies of F_2 computed using CCSD(T) methodology over the exponents of the introduced *d*-type bond-functions. The AO basis was *aug-cc-pwCVQZ* for the F atom.

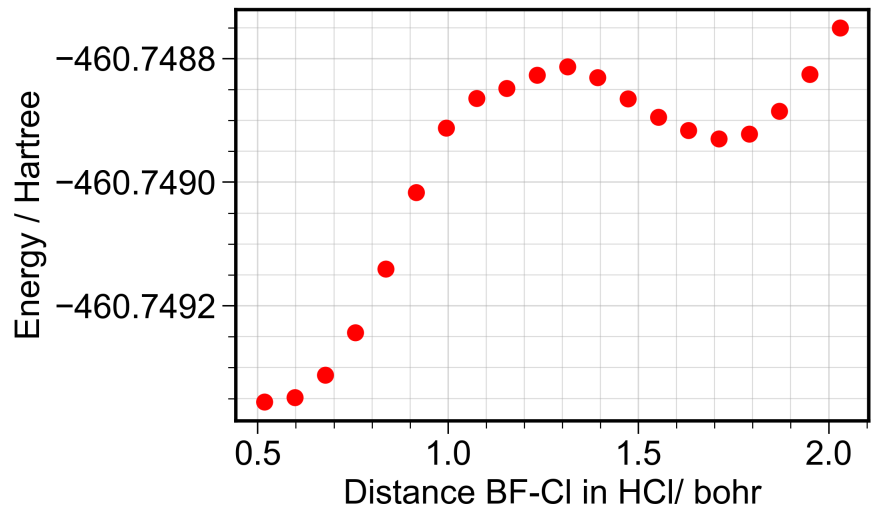

FIG. F21: CCSD(T) energy of the HCl molecule with the introduction of bond-functions at different locations along the inter-nuclear distance. For placing the bond function, the distance of 0.75589 Bohr from the Cl-atom was chosen.

Fig. F22 shows the energy of the HF molecule as the position of the bond-function is changed. The AO basis used in this case is *aug-cc-pVQZ* for the H-atom and *aug-cc-pwCVQZ* for the F atom (from the EMSL database[47]). The bond-function is even-tempered $6s5p4d3f$ composite function (where each functions is constructed as $\alpha\beta^k$, with *s*: α =6.5, β =0.6; *p*: α =5.0, β =0.55; *d*: α =5.125, β =0.6; and *f*: α =4.5937, β =0.42).

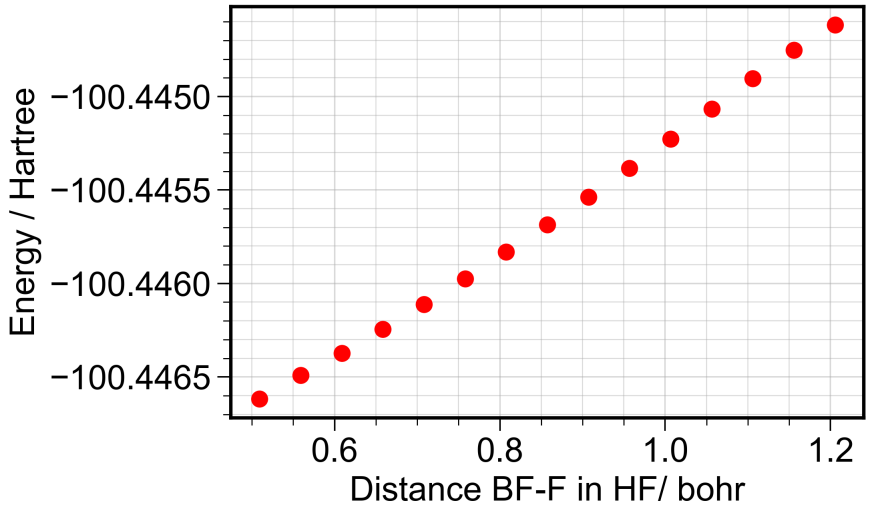

FIG. F22: CCSD(T) energy of the HF molecule with the introduction of bond-functions at different locations along the inter-nuclear distance. Distance of 0.6614 Bohr from the F-atom was chosen for placing the bond-functions in the final computations.

Fig. F23 shows the energy of the N_2 molecule as the position of the bond-function is changed. The AO basis used in this case is *aug-cc-pwCVQZ* (from the EMSL database[47]) while the bond-function is even-tempered $3f$ function (constructed as $\alpha\beta^k$, where α =2.8, β =0.47).

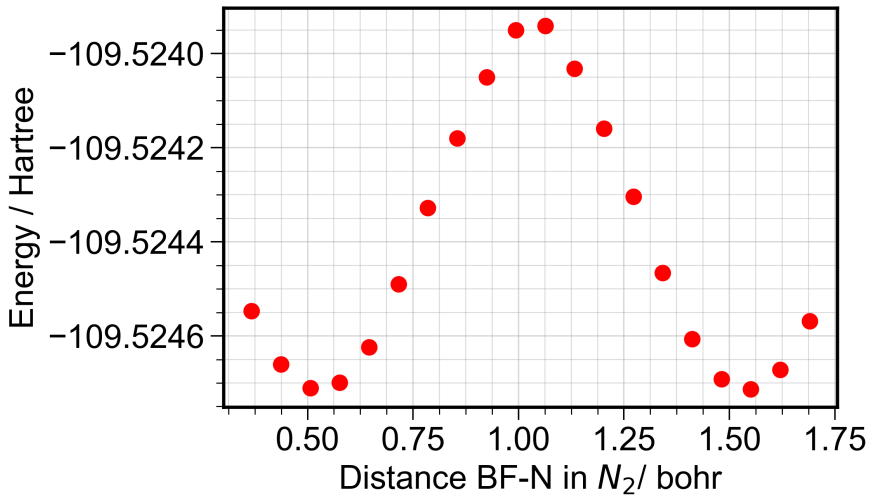

FIG. F23: CCSD(T) energy of the N_2 molecule with the introduction of bond-functions at different locations along the inter-nuclear distance. Distance of 0.5669 Bohr from the N-atom was chosen for placing the bond-functions in the final computations.

Fig. F24 shows the energy of the F_2 molecule as the position of the bond-function is changed. The AO basis used in this case is *aug-cc-pwCVQZ* (from the EMSL database[47]) while the bond-function is even-tempered $1g$ function (constructed as α, where α =1.5).

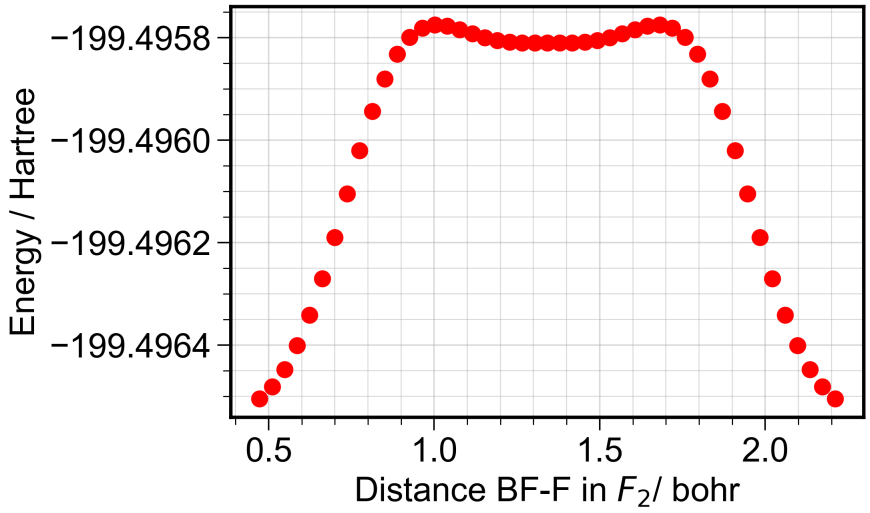

FIG. F24: CCSD(T) energy of the F_2 molecule with the introduction of bond-functions at different locations along the inter-nuclear distance. Distance of 0.4724 Bohr from the F-atom was chosen for placing the bond-functions in the final computations.

TABLE T1: Details on the basis sets including the exponents of the bond-functions used in the present computations with CCSD(T) methodology.

Molecule	**Atomic basis**	**Bond function**	**BF parameters**	
H_2	aug-mcc-pV6Z	8s6p	$\alpha_p = 1.8518519$	$\beta_p = 3.0$
			$\alpha_s = 2.520$	$\beta_s = 3.0$
HF	H:aug-cc-pVQZ, F:aug-cc-pwCVQZ	1×5p4d3f	$\alpha_f = 5.0$	$\beta_f = 0.40$
			$\alpha_d = 5.0$	$\beta_d = 0.60$
			$\alpha_p = 6.5$	$\beta_p = 0.50$
HCl	H:aug-cc-pVQZ, Cl:aug-cc-pwCVQZ	1×5p4d3f	$\alpha_f = 6.0$	$\beta_f = 0.40$
			$\alpha_d = 8.0$	$\beta_d = 0.50$
			$\alpha_p = 5.5$	$\beta_p = 0.60$
CO	C:aug-cc-pVQZ, O:aug-cc-pVQZ	1×5p4d3f	$\alpha_f = 3.0$	$\beta_f = 0.50$
			$\alpha_d = 4.0$	$\beta_d = 0.60$
			$\alpha_p = 5.0$	$\beta_p = 0.50$
N_2	N:aug-cc-pwCVQZ	2×4d3f	$\alpha_f = 2.5$	$\beta_f = 0.50$
			$\alpha_d = 4.5$	$\beta_d = 0.50$
F_2	F:aug-cc-pwCVQZ	2×4d3f2g	$\alpha_g = 4.0$	$\beta_g = 0.40$
			$\alpha_f = 4.0$	$\beta_f = 0.50$
			$\alpha_d = 4.0$	$\beta_d = 0.70$

S3. Results on the polarizability for the selected molecules

A. HF

TABLE T2: Polarizability components ($\alpha_\perp$ and $\alpha_\parallel$) and invariants ($\bar{\alpha}$ and γ) of HF calculated with CCSD(T) methodology and *aug-cc-pwCVQZ* AO basis. All values are in atomic units.

r	$\alpha_\perp$	$\alpha_\parallel$	$\bar{\alpha}$	γ
1.037	4.161783	3.570735	3.964767	-0.591048
1.132	4.283384	3.827015	4.131261	-0.456370
1.226	4.392289	4.100996	4.295191	-0.291293
1.321	4.514122	4.421073	4.483106	-0.093049
1.415	4.637976	4.779894	4.685282	0.141918
1.510	4.763929	5.181203	4.903020	0.417275
1.585	4.866431	5.535708	5.089523	0.669277
1.548	4.815006	5.354604	4.994872	0.539598
1.604	4.892288	5.629247	5.137941	0.736960
1.623	4.918247	5.724830	5.187108	0.806583
1.661	4.970471	5.922265	5.287736	0.951793
1.699	5.023089	6.128284	5.391487	1.105194
1.737	5.076087	6.343163	5.498445	1.267076
1.774	5.129453	6.567191	5.608699	1.437738
1.793	5.156271	6.682727	5.665090	1.526456
1.812	5.183178	6.800662	5.722339	1.617484
1.850	5.237251	7.043875	5.839459	1.806624
1.890	5.294390	7.310067	5.966282	2.015677
1.926	5.346393	7.560748	6.084511	2.214355
1.963	5.401434	7.835041	6.212637	2.433607
1.982	5.429066	7.976295	6.278142	2.547229
2.001	5.456769	8.120343	6.344627	2.663574
2.039	5.512375	8.416971	6.480574	2.904595
2.077	5.568225	8.725230	6.620560	3.157004
2.171	5.708856	9.549228	6.988980	3.840373
2.266	5.850672	10.453954	7.385100	4.603282
2.360	5.993264	11.444985	7.810504	5.451721
2.455	6.136595	12.529239	8.267477	6.392644
2.549	6.279166	13.708645	8.755659	7.429478
2.644	6.459212	15.113611	9.344011	8.654399
2.738	6.565985	16.388222	9.840064	9.822237
2.927	6.847747	19.486240	11.060578	12.638492
2.835	6.709935	17.915356	10.445075	11.205420
3.022	6.986844	21.182614	11.718767	14.195770
3.116	7.124258	22.957645	12.402054	15.833388
3.211	7.259559	24.785508	13.101542	17.525948
3.305	7.392392	26.630064	13.804949	19.237672
3.400	7.522280	28.443542	14.496034	20.921262
3.494	7.648730	30.166814	15.154758	22.518084
3.589	7.771165	31.731064	15.757798	23.959900
3.683	7.888948	33.061054	16.279650	25.172106
3.779	8.003581	34.096694	16.701286	26.093112
3.872	8.107791	34.715723	16.977102	26.607932
3.967	8.207437	34.907146	17.107340	26.699709

TABLE T3: Polarizability components ($\alpha_\perp$ and $\alpha_\parallel$) and invariants ($\bar{\alpha}$ and γ) of HF calculated with with CCSD(T) methodology and *aug-cc-pwCVQZ* AO basis, along with one 5p4d3f bond-function basis. All values are in atomic units. For more details on the exponents of the bond-functions and their location, refer to the Sec. S2 in the supplementary material.

r	$\alpha_\perp$	$\alpha_\parallel$	$\bar{\alpha}$	γ
1.037	4.155248	3.573955	3.961483	-0.581293
1.132	4.275958	3.831072	4.127662	-0.444886
1.226	4.384696	4.105688	4.291694	-0.279008
1.321	4.506889	4.426152	4.479977	-0.080737
1.415	4.631157	4.784906	4.682407	0.153749
1.510	4.757768	5.186126	4.900554	0.428358
1.585	4.860821	5.540503	5.087382	0.679682
1.548	4.809103	5.359441	4.992549	0.550337
1.604	4.886834	5.634015	5.135894	0.747182
1.623	4.912944	5.729565	5.185151	0.816620
1.661	4.965458	5.926916	5.285944	0.961458
1.699	5.018350	6.132836	5.389845	1.114486
1.737	5.071632	6.347611	5.496959	1.275979
1.774	5.125293	6.571530	5.607372	1.446237
1.793	5.152259	6.687003	5.663840	1.534745
1.812	5.179322	6.804875	5.721173	1.625554
1.850	5.233719	7.047949	5.838462	1.814230
1.890	5.291214	7.313964	5.965464	2.022750
1.926	5.343553	7.564457	6.083854	2.220904
1.963	5.398958	7.838519	6.212145	2.439561
1.982	5.426774	7.979642	6.277730	2.552868
2.001	5.454668	8.123534	6.344290	2.668866
2.039	5.510655	8.419858	6.480389	2.909204
2.077	5.566902	8.727824	6.620542	3.160922
2.171	5.708534	9.550976	6.989348	3.842442
2.266	5.851324	10.454845	7.385831	4.603521
2.360	5.994887	11.445470	7.811748	5.450583
2.455	6.138823	12.528984	8.268877	6.390162
2.549	6.282740	13.711246	8.758908	7.428506
2.644	6.462530	15.115194	9.346752	8.652664
2.738	6.569115	16.390509	9.842913	9.821393
2.927	6.851501	19.497624	11.066875	12.646123
2.835	6.713766	17.922792	10.450108	11.209026
3.022	6.990525	21.199591	11.726880	14.209067
3.116	7.127714	22.981437	12.412288	15.853724
3.211	7.262752	24.817864	13.114456	17.555112
3.305	7.395282	26.672863	13.821142	19.277581
3.400	7.524889	28.498810	14.516196	20.973921
3.494	7.651094	30.236618	15.179602	22.585524
3.589	7.773350	31.817321	15.788007	24.043971
3.683	7.891040	33.165331	16.315803	25.274291
3.779	8.005670	34.220188	16.743843	26.214518
3.872	8.109981	34.857909	17.025957	26.747928
3.967	8.209830	35.067757	17.162472	26.857927

B. HCl

TABLE T4: Polarizability components ($\alpha_\perp$ and $\alpha_\parallel$) and invariants ($\bar{\alpha}$ and γ) of HCl calculated with *aug-cc-pwCVQZ* AO basis. All values are in atomic units.

r	$\alpha_\perp$	$\alpha_\parallel$	$\bar{\alpha}$	γ
1.415	15.260194	12.482456	14.334281	-2.777738
1.604	15.508711	13.189690	14.735704	-2.319022
1.699	15.634199	13.605255	14.957884	-2.028944
1.793	15.762962	14.065883	15.197269	-1.697079
1.890	15.898609	14.585196	15.460804	-1.313413
1.982	16.033490	15.134151	15.733710	-0.899340
2.077	16.175886	15.747809	16.033194	-0.428077
2.115	16.234187	16.009052	16.159142	-0.225136
2.152	16.293242	16.279579	16.288688	-0.013663
2.171	16.323048	16.418379	16.354825	0.095331
2.190	16.353037	16.559566	16.421880	0.206529
2.228	16.413554	16.849173	16.558760	0.435619
2.268	16.477852	17.163780	16.706494	0.685928
2.304	16.536672	17.457845	16.843729	0.921174
2.341	16.599224	17.777176	16.991875	1.177952
2.360	16.630738	17.940642	17.067373	1.309904
2.379	16.662404	18.106660	17.143823	1.444255
2.417	16.726178	18.446391	17.299582	1.720213
2.455	16.790504	18.796443	17.459150	2.005939
2.493	16.855342	19.156880	17.622521	2.301538
2.530	16.920658	19.527730	17.789682	2.607072
2.549	16.953484	19.717065	17.874678	2.763580
2.568	16.986418	19.909008	17.960615	2.922591
2.606	17.052580	20.300704	18.135288	3.248123
2.646	17.122430	20.723147	18.322669	3.600716
2.738	17.286600	21.752834	18.775345	4.466235
2.833	17.455199	22.865342	19.258580	5.410143
2.927	17.624032	24.037029	19.761697	6.412997
3.024	17.795517	25.288129	20.293054	7.492612
3.116	17.958636	26.537012	20.818094	8.578376
3.211	18.122447	27.850374	21.365089	9.727927
3.305	18.282539	29.192541	21.919206	10.910002
3.402	18.440940	30.577905	22.486595	12.136965
3.494	18.587473	31.909457	23.028134	13.321984
3.589	18.730292	33.250940	23.570508	14.520649
3.683	18.865436	34.554596	24.095156	15.689159
3.779	18.994432	35.821250	24.603371	16.826818
3.872	19.109216	36.953241	25.057224	17.844025
3.967	19.216447	37.995301	25.476065	18.778853
4.061	19.313169	38.894694	25.840344	19.581525
4.157	19.400619	39.635079	26.145439	20.234461
4.250	19.473739	40.150688	26.366055	20.676949
4.344	19.539983	40.453798	26.511255	20.913815
4.439	19.591057	40.510122	26.564078	20.919065

TABLE T5: Polarizability components ($\alpha_\perp$ and $\alpha_\parallel$) and invariants ($\bar{\alpha}$ and γ) of HCl calculated with CCSD(T) methodology and *aug-cc-pwCVQZ* AO basis along with one 5p4d3f bond-function basis. All values are in atomic units. For more details on the exponents of the bond-functions and their location, refer to the Sec. S2 in the supplementary material.

r	$\alpha_\perp$	$\alpha_\parallel$	$\bar{\alpha}$	γ
1.415	15.116577	12.176866	14.321517	-2.769859
1.604	15.244803	12.474944	14.722271	-2.307635
1.699	15.491482	13.183847	14.944296	-2.016950
1.793	15.616612	13.599662	15.183548	-1.685093
1.890	15.745246	14.060152	15.446958	-1.301952
1.982	15.880942	14.578990	15.719748	-0.888761
2.077	16.016002	15.127241	16.019129	-0.418740
2.115	16.158709	15.739969	16.145033	-0.216355
2.152	16.217151	16.000796	16.274552	-0.005507
2.171	16.276387	16.270881	16.340668	0.103180
2.190	16.306275	16.409455	16.407702	0.214061
2.228	16.336348	16.550409	16.544542	0.442497
2.268	16.397043	16.839540	16.692248	0.692066
2.304	16.461559	17.153625	16.829453	0.926633
2.341	16.520575	17.447208	16.977564	1.182695
2.360	16.583332	17.766027	17.053045	1.314286
2.379	16.614950	17.929235	17.129479	1.448272
2.417	16.646721	18.094994	17.285229	1.723456
2.455	16.710744	18.434200	17.444782	2.008441
2.493	16.775302	18.783742	17.608152	2.303288
2.530	16.840390	19.143677	17.775347	2.608038
2.549	16.906001	19.514039	17.860356	2.764181
2.568	16.938962	19.703143	17.946307	2.922830
2.606	16.972030	19.894860	18.121020	3.247663
2.646	17.038466	20.286129	18.308476	3.599533
2.738	17.108632	20.708165	18.761397	4.463578
2.833	17.273538	21.737116	19.245057	5.406317
2.927	17.442952	22.849268	19.748799	6.408521
3.024	17.612626	24.021147	20.281048	7.488203
3.116	17.784980	25.273184	20.807247	8.574948
3.211	17.948931	26.523879	21.355786	9.726618
3.305	18.113580	27.840198	21.911938	10.912313
3.402	18.274501	29.186814	22.481991	12.144840
3.494	18.433711	30.578551	23.026755	13.337305
3.589	18.580987	31.918291	23.573201	14.545904
3.683	18.724566	33.270470	24.102763	15.726968
3.779	18.860440	34.587408	24.616981	16.880321
3.872	18.990208	35.870528	25.077542	17.915377
3.967	19.105750	37.021127	25.504123	18.870968
4.061	19.213801	38.084769	25.876955	19.696716
4.157	19.311383	39.008099	26.191450	20.375092
4.250	19.399752	39.774844	26.421534	20.843089
4.344	19.473837	40.316927	26.576474	21.106044
4.439	19.541126	40.647170	26.638664	21.136832

C. CO

TABLE T6: Polarizability components ($\alpha_\perp$ and $\alpha_\parallel$) and invariants ($\bar{\alpha}$ and γ) of CO calculated with *aug-cc-pwCVQZ* AO basis and CCSD(T) method. All values are in atomic units.

r	$\alpha_\perp$	$\alpha_\parallel$	$\bar{\alpha}$	γ
1.308	10.130278	9.256813	9.839123	-0.873465
1.402	10.279187	9.673707	10.077360	-0.605480
1.497	10.440939	10.176603	10.352827	-0.264336
1.587	10.609872	10.732592	10.650779	0.122721
1.682	10.796547	11.384889	10.992661	0.588342
1.776	10.996077	12.111498	11.367884	1.115421
1.871	11.209045	12.913669	11.777253	1.704624
1.907	11.293047	13.238641	11.941578	1.945594
1.945	11.382664	13.592850	12.119393	2.210186
1.962	11.423523	13.756322	12.201123	2.332799
1.982	11.474060	13.959571	12.302563	2.485511
2.018	11.563267	14.319600	12.482045	2.756333
2.056	11.659856	14.710848	12.676853	3.050992
2.094	11.758638	15.114644	12.877307	3.356006
2.130	11.854019	15.509830	13.072623	3.655811
2.151	11.909880	15.743757	13.187839	3.833876
2.168	11.955941	15.937940	13.283274	3.981999
2.205	12.059471	16.378411	13.499118	4.318939
2.245	12.169872	16.854025	13.731256	4.684153
2.281	12.271111	17.295643	13.945955	5.024532
2.319	12.378916	17.771815	14.176549	5.392898
2.336	12.427806	17.989812	14.281808	5.562005
2.356	12.487855	18.259347	14.411686	5.771492
2.392	12.592280	18.732823	14.639127	6.140543
2.430	12.703048	19.241871	14.882656	6.538823
2.525	12.982757	20.561008	15.508840	7.578251
2.619	13.264463	21.946472	16.158466	8.682009
2.710	13.534515	23.345076	16.804702	9.810562
2.804	13.813313	24.894484	17.507037	11.081171
2.899	14.088070	26.588996	18.255045	12.500927
2.993	14.358632	28.536973	19.084745	14.178341
3.084	14.616703	30.848825	20.027410	16.232122
3.179	14.890827	34.135257	21.305637	19.244430
3.273	15.184793	39.108722	23.159436	23.923929
3.367	15.518476	47.026613	26.021188	31.508137
3.458	15.888725	58.813973	30.197141	42.925248
3.553	16.323361	76.848136	36.498286	60.524775
3.647	16.792300	101.951262	45.178621	85.158962
3.742	17.277950	134.732577	56.429493	117.454627
3.832	17.745817	173.382708	69.624780	155.636892
3.927	18.220395	221.034509	85.825100	202.814115
4.021	18.667141	276.138617	104.490966	257.471475

TABLE T7: Polarizability components ($\alpha_\perp$ and $\alpha_\parallel$) and invariants ($\bar{\alpha}$ and γ) of CO calculated with CCSD(T) methodology and *aug-cc-pwCVQZ* AO basis along with one 5p4d3f bond-function basis. All values are in atomic units. For more details on the exponents of the bond-functions and their location, refer to the Sec. S2 in the supplementary material.

r	$\alpha_\perp$	$\alpha_\parallel$	$\bar{\alpha}$	γ
1.308	10.125301	9.250433	9.833678	-0.874868
1.402	10.274084	9.666054	10.071408	-0.608030
1.497	10.435802	10.167510	10.346371	-0.268292
1.587	10.604777	10.721974	10.643843	0.117196
1.682	10.791353	11.372666	10.985124	0.581313
1.776	10.990689	12.097821	11.359733	1.107131
1.871	11.202980	12.898759	11.768239	1.695779
1.907	11.287040	13.223310	11.932463	1.936270
1.945	11.377521	13.577067	12.110703	2.199546
1.962	11.418898	13.740329	12.192708	2.321431
1.982	11.467057	13.943325	12.292480	2.476268
2.018	11.556821	14.302891	12.472178	2.746069
2.056	11.653211	14.693597	12.666673	3.040386
2.094	11.751492	15.096827	12.866604	3.345335
2.130	11.846546	15.491462	13.061518	3.644916
2.151	11.902303	15.725051	13.176552	3.822748
2.168	11.948306	15.918938	13.271850	3.970632
2.205	12.051719	16.358947	13.487462	4.307228
2.245	12.161963	16.833781	13.719236	4.671818
2.281	12.263069	17.274713	13.933617	5.011645
2.319	12.370769	17.750251	14.163930	5.379481
2.336	12.419626	17.967993	14.269082	5.548368
2.356	12.479643	18.237247	14.398844	5.757604
2.392	12.584030	18.710281	14.626114	6.126251
2.430	12.694779	19.218898	14.869485	6.524120
2.525	12.974535	20.537223	15.495431	7.562687
2.619	13.256424	21.922250	16.145033	8.665826
2.710	13.526762	23.320704	16.791409	9.793942
2.804	13.805955	24.870096	17.494002	11.064141
2.899	14.081183	26.564512	18.242293	12.483329
2.993	14.352274	28.511950	19.072166	14.159676
3.084	14.610886	30.822271	20.014681	16.211385
3.179	14.885591	34.104765	21.291982	19.219174
3.273	15.180087	39.067993	23.142723	23.887906
3.367	15.514297	46.966709	25.998434	31.452412
3.458	15.885177	58.724554	30.164969	42.839378
3.553	16.320448	76.714849	36.451915	60.394401
3.647	16.789006	101.733463	45.103825	84.944456
3.742	17.276971	134.475246	56.343062	117.198276
3.832	17.746139	172.772151	69.421476	155.026012
3.927	18.227509	217.330610	84.595210	199.103101
4.021	18.699595	261.154286	99.517826	242.454691

D. N_2

TABLE T8: Polarizability components ($\alpha_\perp$ and $\alpha_\parallel$) and invariants ($\bar{\alpha}$ and γ) of N_2 calculated with *aug-cc-pwCVQZ* AO basis and CCSD(T) methodology. All values are in atomic units.

r	$\alpha_\perp$	$\alpha_\parallel$	$\bar{\alpha}$	γ
1.319	7.735958	8.474836	7.982251	0.738877
1.415	7.981491	8.988031	8.317004	1.006540
1.510	8.251190	9.593616	8.698665	1.342426
1.602	8.537133	10.268138	9.114135	1.731005
1.697	8.846570	11.024075	9.572405	2.177505
1.737	8.980952	11.358627	9.773511	2.377675
1.773	9.104465	11.668816	9.959249	2.564352
1.793	9.176732	11.851371	10.068278	2.674639
1.812	9.242875	12.019080	10.168276	2.776205
1.848	9.369614	12.341958	10.360396	2.972343
1.890	9.517906	12.722005	10.585939	3.204099
1.926	9.647094	13.054826	10.783005	3.407731
1.962	9.777127	13.391246	10.981833	3.614119
1.980	9.845842	13.569544	11.087076	3.723703
2.001	9.921608	13.766518	11.203244	3.844910
2.037	10.052820	14.108487	11.404709	4.055667
2.064	10.149694	14.361574	11.553654	4.211881
2.077	10.198166	14.488383	11.628239	4.290217
2.113	10.329768	14.833187	11.830908	4.503420
2.152	10.475117	15.214813	12.055015	4.739696
2.171	10.544228	15.396535	12.161664	4.852307
2.188	10.606343	15.559996	12.257561	4.953653
2.228	10.750867	15.940740	12.480824	5.189873
2.264	10.880985	16.283925	12.681965	5.402940
2.304	11.023894	16.661126	12.902971	5.637232
2.339	11.152213	16.999941	13.101456	5.847728
2.360	11.226018	17.194825	13.215620	5.968806
2.379	11.292777	17.371080	13.318878	6.078303
2.415	11.418655	17.703308	13.513539	6.284653
2.455	11.556171	18.065954	13.726099	6.509783
2.547	11.869548	18.889859	14.209651	7.020311
2.642	12.176782	19.691160	14.681574	7.514379
2.738	12.474838	20.457416	15.135697	7.982579
2.835	12.758721	21.160524	15.559322	8.401804
2.925	13.005080	21.752259	15.920806	8.747178
3.022	13.245361	22.290438	16.260387	9.045077
3.116	13.456986	22.707135	16.540369	9.250149
3.209	13.638493	22.983406	16.753464	9.344913
3.305	13.796754	23.096498	16.896669	9.299744
3.400	13.917318	22.987086	16.940574	9.069768
3.492	14.003420	22.605511	16.870784	8.602091
3.587	14.041577	21.846973	16.643375	7.805397
3.683	14.028448	20.556164	16.204353	6.527716
3.779	13.957035	18.550155	15.488075	4.593120
3.870	13.832969	15.772198	14.479379	1.939229

TABLE T9: Polarizability components ($\alpha_\perp$ and $\alpha_\parallel$) and invariants ($\bar{\alpha}$ and γ) of N_2 calculated with CCSD(T) *aug-cc-pwCVQZ* AO basis along with one 4d3f bond-function basis. All values are in atomic units. For more details on the exponents of the bond-functions and their location, refer to the Sec. S2 in the supplementary material.

r	$\alpha_\perp$	$\alpha_\parallel$	$\bar{\alpha}$	γ
1.319	7.736587	8.469563	7.980913	0.732976
1.415	7.981456	8.982253	8.315055	1.000798
1.510	8.250532	9.587235	8.696100	1.336703
1.602	8.535759	10.260996	9.110838	1.725237
1.697	8.844355	11.016101	9.568270	2.171746
1.737	8.978350	11.350307	9.769002	2.371957
1.773	9.101491	11.660183	9.954388	2.558692
1.793	9.173542	11.842562	10.063216	2.669020
1.812	9.239494	12.010121	10.163036	2.770626
1.848	9.365857	12.332716	10.354810	2.966858
1.890	9.513728	12.712460	10.579972	3.198732
1.926	9.642567	13.045045	10.776726	3.402477
1.962	9.772272	13.381247	10.975264	3.608975
1.980	9.840831	13.559444	11.080369	3.718612
2.001	9.916430	13.756306	11.196389	3.839876
2.037	10.047375	14.098104	11.397618	4.050729
2.064	10.144075	14.351096	11.546415	4.207021
2.077	10.192467	14.477869	11.620934	4.285403
2.113	10.323864	14.822480	11.823402	4.498616
2.152	10.469023	15.204094	12.047380	4.735072
2.171	10.538055	15.385818	12.153976	4.847763
2.188	10.600096	15.549269	12.249820	4.949173
2.228	10.744476	15.930008	12.472987	5.185532
2.264	10.874473	16.273201	12.674049	5.398728
2.304	11.017264	16.650462	12.894997	5.633198
2.339	11.145471	16.989370	13.093437	5.843899
2.360	11.219211	17.184324	13.207582	5.965113
2.379	11.285911	17.360654	13.310825	6.074743
2.415	11.411666	17.693051	13.505461	6.281385
2.455	11.549053	18.055930	13.718012	6.506876
2.547	11.862077	18.880584	14.201579	7.018507
2.642	12.168923	19.682964	14.673603	7.514042
2.738	12.466738	20.450680	15.128052	7.983942
2.835	12.750441	21.155651	15.552178	8.405210
2.925	12.996874	21.749585	15.914444	8.752711
3.022	13.237555	22.290696	16.255268	9.053141
3.116	13.449829	22.711046	16.536901	9.261217
3.209	13.632262	22.991920	16.752148	9.359658
3.305	13.791750	23.111268	16.898256	9.319517
3.400	13.913946	23.010016	16.945969	9.096070
3.492	14.001925	22.639220	16.881023	8.637295
3.587	14.042095	21.895626	16.659938	7.853531
3.683	14.031646	20.625866	16.229719	6.594220
3.779	13.963198	18.648845	15.525080	4.685647
3.870	13.842086	15.907065	14.530413	2.064979

E. F_2

TABLE T10: Polarizability components ($\alpha_\perp$ and $\alpha_\parallel$) and invariants ($\bar{\alpha}$ and γ) of F_2 calculated with *aug-cc-pwCVQZ* AO basis and CCSD(T) methodology. All values are in atomic units.

r	$\alpha_\perp$	$\alpha_\parallel$	$\bar{\alpha}$	γ
1.319	9.133620	15.746775	11.338005	6.613156
1.414	7.261062	11.293301	8.605141	4.032240
1.512	6.289417	8.946412	7.175082	2.656995
1.604	5.824352	7.807530	6.485412	1.983178
1.701	5.587415	7.238976	6.137936	1.651560
1.793	5.497662	7.071003	6.022109	1.573341
1.890	5.491268	7.171676	6.051404	1.680408
1.984	5.538974	7.475532	6.184494	1.936558
2.079	5.620094	7.936555	6.392248	2.316461
2.169	5.717200	8.491928	6.642109	2.774727
2.266	5.831939	9.167695	6.943858	3.335756
2.360	5.949600	9.880800	7.260000	3.931200
2.457	6.070198	10.623237	7.587878	4.553038
2.551	6.185836	11.330932	7.900868	5.145096
2.642	6.292467	11.960817	8.181917	5.668349
2.683	6.339469	12.225716	8.301551	5.886247
2.736	6.397632	12.536074	8.443780	6.138442
2.833	6.498752	13.010446	8.669317	6.511694
2.927	6.589715	13.342715	8.840715	6.753000
3.024	6.675042	13.528667	8.959583	6.853625
3.116	6.750132	13.551401	9.017222	6.801270
3.209	6.818822	13.419051	9.018898	6.600228
3.303	6.882835	13.123774	8.963148	6.240938
3.402	6.943593	12.656238	8.847808	5.712645
3.496	6.997199	12.067845	8.687414	5.070646
3.589	7.045944	11.378078	8.489989	4.332133
3.683	7.092631	10.580819	8.255360	3.488188
3.779	7.137879	9.694938	7.990232	2.557059
3.870	7.178915	8.816507	7.724779	1.637593
3.968	7.222199	7.839361	7.427920	0.617162
4.059	7.261335	6.932736	7.151802	-0.328599
4.157	7.302851	5.963414	6.856372	-1.339438
4.250	7.340867	5.075708	6.585814	-2.265159
4.344	7.378032	4.205977	6.320680	-3.172055
4.441	7.413507	3.363955	6.063656	-4.049552
4.532	7.443887	2.617409	5.835061	-4.826478

TABLE T11: Polarizability components ($\alpha_\perp$ and $\alpha_\parallel$) and invariants ($\bar{\alpha}$ and γ) of F_2 calculated with CCSD(T) methodology and *aug-cc-pwCVQZ* AO basis along with one 4d3f2g bond-function basis. All values are in atomic units. For more details on the exponents of the bond-functions and their location, refer to the Sec. S2 in the supplementary material.

r	$\alpha_\perp$	$\alpha_\parallel$	$\bar{\alpha}$	γ
1.319	9.159092	15.741901	11.353362	6.582809
1.414	7.271567	11.284708	8.609281	4.013142
1.512	6.295472	8.943606	7.178183	2.648134
1.604	5.827403	7.805827	6.486878	1.978424
1.701	5.588401	7.237902	6.138235	1.649501
1.793	5.497052	7.070289	6.021464	1.573237
1.890	5.489180	7.171213	6.049857	1.682033
1.984	5.535526	7.475252	6.182101	1.939727
2.079	5.615416	7.936479	6.389104	2.321063
2.169	5.711554	8.492158	6.638422	2.780605
2.266	5.825555	9.168444	6.939851	3.342889
2.360	5.942816	9.882328	7.255987	3.939513
2.457	6.063313	10.625909	7.584179	4.562596
2.551	6.179038	11.335110	7.897729	5.156072
2.642	6.285746	11.966887	8.179460	5.681141
2.683	6.332839	12.232836	8.299504	5.899997
2.736	6.391099	12.544538	8.442246	6.153439
2.833	6.492594	13.021560	8.668916	6.528966
2.927	6.584111	13.356380	8.841534	6.772270
3.024	6.670135	13.544652	8.961641	6.874517
3.116	6.745945	13.569151	9.020347	6.823206
3.209	6.815362	13.437936	9.022887	6.622574
3.303	6.880180	13.142816	8.967726	6.262636
3.402	6.941858	12.674413	8.852709	5.732555
3.496	6.996453	12.084048	8.692318	5.087595
3.589	7.046317	11.391217	8.494617	4.344901
3.683	7.094334	10.589671	8.259446	3.495337
3.779	7.141154	9.698278	7.993528	2.557124
3.870	7.183890	8.813708	7.727162	1.629819
3.968	7.229306	7.829052	7.429221	0.599746
4.059	7.270685	6.914883	7.152085	-0.355802
4.157	7.314960	5.936981	6.855634	-1.377979
4.250	7.355878	5.040991	6.584249	-2.314888
4.344	7.396261	4.162812	6.318444	-3.233449
4.441	7.435199	3.312286	6.060895	-4.122912
4.532	7.468890	2.557916	5.831899	-4.910974

F. Polarizability computed using different *ab initio* techniques

TABLE T12: Static (wavelength independent) polarizability components for the HF molecule computed with Hartree-Fock, DFT, CASSCF, CCSD(T) methods. The basis set used in these calculations was *aug-cc-pVQZ*.

	HF		DFT		CASSCF		CCSD(T)	
r	$\alpha_\perp$	$\alpha_\parallel$	$\alpha_\perp$	$\alpha_\parallel$	$\alpha_\perp$	$\alpha_\parallel$	$\alpha_\perp$	$\alpha_\parallel$
0.992	3.6687	3.1304	4.3781	3.6557	3.6786	3.1414	3.4892	2.6363
1.087	3.7653	3.3429	4.4987	3.9071	3.7683	3.3570	3.6469	2.7901
1.181	3.8600	3.5820	4.6179	4.1876	3.8613	3.5980	3.7874	2.9575
1.276	3.9541	3.8519	4.7369	4.5005	3.9533	3.8757	3.9176	3.1419
1.370	4.0484	4.1571	4.8563	4.8487	4.0459	4.1980	4.0422	3.3468
1.465	4.1438	4.5023	4.9766	5.2353	4.1395	4.5653	4.1034	3.4580
1.559	4.2410	4.8925	5.0979	5.6632	4.2347	4.9894	4.1643	3.5757
1.654	4.3404	5.3329	5.2204	6.1348	4.3322	5.4754	4.2250	3.7003
1.748	4.4424	5.8287	5.3441	6.6524	4.4324	6.0327	4.2856	3.8323
1.842	4.5475	6.3850	5.4689	7.2180	4.5359	6.6687	4.3464	3.9721
1.937	4.6557	7.0070	5.5947	7.8329	4.6433	7.3890	4.3946	4.1069
2.031	4.7672	7.6994	5.7214	8.4982	4.7552	8.1973	4.4554	4.2628
2.126	4.8821	8.4667	5.8487	9.2143	4.8720	9.0934	4.5166	4.4279
2.220	5.0004	9.3130	5.9765	9.9811	4.9943	10.0718	4.5783	4.6026
2.315	5.1220	10.2418	6.1046	10.7984	5.1224	11.1201	4.6405	4.7875
2.409	5.2468	11.2563	6.2327	11.6651	5.2565	12.2177	4.7032	4.9830
2.504	5.3744	12.3592	6.3607	12.5800	5.3965	13.3354	4.7665	5.1897
2.598	5.5046	13.5529	6.4881	13.5416	5.5419	14.4366	4.8304	5.4081
2.693	5.6371	14.8391	6.6148	14.5481	5.6918	15.4793	4.8949	5.6387
2.787	5.7714	16.2193	6.7402	15.5973	5.8449	16.4205	4.9600	5.8821
2.882	5.9070	17.6944	6.8642	16.6869	5.9996	17.2209	5.0257	6.1388
2.976	6.0436	19.2648	6.9865	17.8144	6.1540	17.8496	5.0920	6.4094
3.071	6.1807	20.9306	7.1066	18.9773	6.3058	18.2873	5.1589	6.6944
3.165	6.3179	22.6913	7.2243	20.1728	6.4531	18.5276	5.2264	6.9944
3.260	6.4547	24.5460	7.3393	21.3981	6.5939	18.5768	5.2944	7.3101
3.354	6.5906	26.4932	7.4514	22.6506	6.7265	18.4512	5.3629	7.6419
3.449	6.7254	28.5313	7.5602	23.9276	6.8497	18.1744	5.4318	7.9906
3.543	6.8585	30.6581	7.6656	25.2269	6.9627	17.7739	5.5012	8.3567
3.638	6.9895	32.8708	7.7673	26.5460	7.0651	17.2783	5.5710	8.7410
3.732	7.1182	35.1666	7.8651	27.8833	7.1569	16.7154	5.6412	9.1440
3.827	7.2441	37.5422	7.9590	29.2368	7.2383	16.1102	5.7117	9.5665
3.921	7.3669	39.9942	8.0487	30.6049	7.3099	15.4846	5.7825	10.0092
4.016	7.4864	42.5189	8.1342	31.9865	7.3725	14.8564	5.8535	10.4729
4.110	7.6023	45.1123	8.2155	33.3805	7.4269	14.2400	5.9247	10.9582
4.205	7.7144	47.7707	8.2925	34.7859	7.4740	13.6460	5.9961	11.4659
4.535	8.0742	57.5290	8.5282	39.7860	7.5932	11.8311	6.0677	11.9967

TABLE T13: Static (wavelength independent) polarizability components for the HCl molecule computed with Hartree-Fock, DFT, CASSCF, CCSD(T) methods. The basis set used in these calculations was *aug-cc-pVQZ*.

	HF		DFT		CASSCF		CCSD(T)	
r	$\alpha_\perp$	$\alpha_\parallel$	$\alpha_\perp$	$\alpha_\parallel$	$\alpha_\perp$	$\alpha_\parallel$	$\alpha_\perp$	$\alpha_\parallel$
0.567	12.3414	10.8695	10.8523	10.7639	12.0253	10.6060	12.6958	11.2430
0.661	12.8144	10.8052	11.3888	10.8395	12.7196	10.7093	13.1609	11.1613
0.756	13.2995	10.8147	11.8826	10.9132	13.2736	10.8245	13.6382	11.1430
0.850	13.7250	10.9033	12.3358	10.9856	13.7078	10.9547	14.0531	11.2069
0.945	14.0634	11.0451	12.7504	11.0573	14.0427	11.1034	14.3816	11.3312
1.039	14.3216	11.2201	13.1285	11.1289	14.2990	11.2737	14.6339	11.4971
1.134	14.5199	11.4198	13.4722	11.2009	14.4973	11.4690	14.8311	11.6964
1.228	14.6782	11.6436	13.7836	11.2740	14.6568	11.6872	14.9927	11.9275
1.323	14.8111	11.8946	14.0647	11.3489	14.7890	11.9063	15.1333	12.1909
1.417	14.9286	12.1763	14.3177	11.4260	14.9096	12.1919	15.2627	12.4888
1.512	15.0375	12.4919	14.5446	11.5060	15.0231	12.5118	15.3874	12.8234
1.606	15.1425	12.8443	14.7475	11.5896	15.1290	12.8513	15.5112	13.1976
1.701	15.2465	13.2372	14.9285	11.6772	15.2334	13.2609	15.6367	13.6140
1.795	15.3517	13.6744	15.0897	11.7696	15.3353	13.6960	15.7656	14.0756
1.890	15.4591	14.1600	15.2331	11.8673	15.4357	14.1574	15.8986	14.5852
1.984	15.5698	14.6989	15.3609	11.9709	15.5406	14.6932	16.0363	15.1459
2.079	15.6842	15.2960	15.4750	12.0811	15.6474	15.2772	16.1788	15.7607
2.173	15.8030	15.9567	15.5777	12.1984	15.7569	15.9189	16.3260	16.4324
2.268	15.9265	16.6866	15.6709	12.3234	15.8690	16.6175	16.4779	17.1638
2.362	16.0551	17.4913	15.7567	12.4568	15.9835	17.3752	16.6339	17.9571
2.457	16.1891	18.3765	15.8372	12.5991	16.1005	18.1942	16.7937	18.8142
2.551	16.3286	19.3479	15.9134	12.7509	16.2198	19.0758	16.9568	19.7361
2.646	16.4737	20.4110	15.9865	12.9126	16.3413	20.0185	17.1224	20.7231
2.740	16.6244	21.5709	16.0573	13.0846	16.4646	21.0183	17.2900	21.7745
2.835	16.7807	22.8325	16.1266	13.2671	16.5893	22.0687	17.4586	22.8882
2.929	16.9424	24.2001	16.1949	13.4605	16.7151	23.1599	17.6274	24.0610
3.024	17.1093	25.6774	16.2628	13.6652	16.8413	24.2792	17.7955	25.2881
3.118	17.2813	27.2676	16.3306	13.8814	16.9675	25.4110	17.9619	26.5629
3.213	17.4579	28.9731	16.3986	14.1096	17.0929	26.5366	18.1257	27.8770
3.307	17.6389	30.7957	16.4670	14.3500	17.2168	27.6350	18.2857	29.2196
3.402	17.8239	32.7367	16.5359	14.6033	17.3387	28.6835	18.4409	30.5779
3.496	18.0122	34.7963	16.6054	14.8696	17.4577	29.6584	18.5904	31.9365
3.590	18.2036	36.9743	16.6756	15.1495	17.5731	30.5362	18.7331	33.2775
3.685	18.3974	39.2700	16.7465	15.4434	17.6842	31.2951	18.8681	34.5801
3.779	18.5930	41.6818	16.8182	15.7517	17.7905	31.9161	18.9944	35.8212
3.874	18.7900	44.2078	16.8907	16.0748	17.8912	32.3842	19.1115	36.9753
3.968	18.9878	46.8455	16.9640	16.4131	17.9860	32.6899	19.2185	38.0148
4.063	19.1858	49.5920	17.0380	16.7671	18.0744	32.8292	19.3150	38.9110
4.157	19.3833	52.4439	17.1129	17.1372	18.1563	32.8044	19.4006	39.6351
4.252	19.5799	55.3975	17.1885	17.5237	18.2315	32.6235	19.4752	40.1590
4.346	19.7749	58.4491	17.2650	17.9271	18.3000	32.2996	19.5412	40.4574
4.441	19.9680	61.5943	17.3421	18.3477	18.3620	31.8502	19.5919	40.5086

TABLE T14: Static (wavelength independent) polarizability components for the CO molecule computed with Hartree-Fock, DFT, CASSCF, CCSD(T) methods. The basis set used in these calculations was *aug-cc-pVQZ*.

	HF		DFT		CASSCF		CCSD(T)	
r	$\alpha_\perp$	$\alpha_\parallel$	$\alpha_\perp$	$\alpha_\parallel$	$\alpha_\perp$	$\alpha_\parallel$	$\alpha_\perp$	$\alpha_\parallel$
0.945	9.0440	8.5433	10.6096	9.9178	7.5616	8.5094	9.9314	9.5167
1.039	9.4086	8.6251	10.5802	9.5434	10.3568	9.0491	9.8244	8.8085
1.228	9.5189	8.6915	10.6431	9.5200	9.7979	8.8822	10.0167	8.9852
1.308	9.5879	8.8959	10.7078	9.7312	9.6869	9.0530	10.1303	9.2568
1.402	9.7261	9.2914	10.8065	10.1012	9.9443	9.4529	10.2792	9.6737
1.497	9.8624	9.7388	10.9233	10.5622	10.0857	10.1456	10.4409	10.1766
1.591	10.0193	10.2621	11.0565	11.0995	10.2330	10.6226	10.6171	10.7573
1.686	10.1926	10.8483	11.2062	11.7091	10.3721	10.8441	10.8043	11.4125
1.720	10.2597	11.0751	11.2641	11.9456	10.4476	11.1009	10.8748	11.6666
1.780	10.3852	11.4984	11.3723	12.3879	10.5880	11.5900	11.0043	12.1421
1.814	10.4592	11.7477	11.4361	12.6488	10.6651	11.8442	11.0796	12.4232
1.909	10.6782	12.4835	11.6242	13.4189	10.8883	12.5935	11.2975	13.2561
2.003	10.9162	13.2830	11.8277	14.2568	11.1280	13.4334	11.5254	14.1666
2.098	11.1724	14.1467	12.0461	15.1633	11.3795	14.3397	11.7686	15.1557
2.192	11.4450	15.0746	12.2780	16.1384	11.6421	15.3209	12.0231	16.2228
2.287	11.7321	16.0661	12.5222	17.1815	11.9134	16.3744	12.2872	17.3663
2.381	12.0310	17.1194	12.7769	18.2902	12.1907	17.4991	12.5592	18.5822
2.476	12.3389	18.2314	13.0405	19.4612	12.4711	18.6918	12.8369	19.8669
2.570	12.6523	19.3971	13.3107	20.6895	12.7516	19.9480	13.1179	21.2176
2.665	12.9674	20.6096	13.5853	21.9693	13.0291	21.2614	13.3997	22.6366
2.759	13.2797	21.8598	13.8620	23.2939	13.3003	22.6246	13.6799	24.1368
2.853	13.5838	23.1362	14.1387	24.6564	13.5623	24.0282	13.9567	25.7527
2.948	13.8731	24.4260	14.4131	26.0504	13.8122	25.4608	14.2292	27.5603
3.042	14.1389	25.7182	14.6830	27.4697	14.0478	26.9079	14.4983	29.7172
3.137	14.3696	27.0136	14.9465	28.9094	14.2670	28.3515	14.7688	32.5405
3.231	14.5519	28.3408	15.2021	30.3652	14.4682	29.7697	15.0518	36.6435
3.326	14.6757	29.7458	15.4485	31.8338	14.6506	31.1372	15.3655	43.0838
3.420	14.7437	31.1952	15.6846	33.3129	14.8141	32.4270	15.7283	53.3145
3.515	14.7731	32.5535	15.9097	34.8010	14.9587	33.6120	16.1443	68.8489
3.590	14.7824	33.4995	16.0817	35.9972	15.0616	34.4679	16.5079	85.9844
3.628	14.7851	33.9194	16.1649	36.5971	15.1089	34.8610	16.6967	96.3117
3.666	14.7874	34.3055	16.2463	37.1983	15.1535	35.2289	16.8880	107.8764
3.704	14.7898	34.6596	16.3258	37.8006	15.1956	35.5701	17.0827	120.6993
3.742	14.7926	34.9840	16.4035	38.4041	15.2353	35.8832	17.2781	134.7683
3.779	14.7962	35.2809	16.4794	39.0089	15.2726	36.1669	17.4735	150.0270
3.817	14.8008	35.5522	16.5535	39.6148	15.3076	36.4196	17.6683	166.3629
3.855	14.8064	35.7994	16.6257	40.2221	15.3405	36.6399	17.8619	183.5949
3.893	14.8132	36.0242	16.6961	40.8306	15.3714	36.8263	18.0539	201.4630
3.931	14.8213	36.2276	16.7647	41.4405	15.4002	36.9772	18.2441	219.6222
3.968	14.8306	36.4105	16.8315	42.0518	15.4273	37.0910	18.4327	237.6417

TABLE T15: Static (wavelength independent) polarizability components for the N_2 molecule computed with Hartree-Fock, DFT, CASSCF, CCSD(T) methods. The basis set used in these calculations was *aug-cc-pVQZ*.

	HF		DFT		CASSCF		CCSD(T)	
r	$\alpha_\perp$	$\alpha_\parallel$	$\alpha_\perp$	$\alpha_\parallel$	$\alpha_\perp$	$\alpha_\parallel$	$\alpha_\perp$	$\alpha_\parallel$
0.945	7.2283	8.0520	13.8899	16.8560	7.0095	7.8617	7.7758	8.5441
1.039	6.6750	7.4453	12.7266	15.3574	6.8622	7.4885	7.3870	7.8970
1.134	6.9337	7.6048	11.7153	14.0340	6.9242	7.5119	7.4019	7.8848
1.228	6.9941	7.7934	10.8462	12.8768	7.0726	7.7314	7.5426	8.1099
1.323	7.2171	8.2020	10.1094	11.8765	7.2666	8.0906	7.7449	8.4927
1.417	7.4380	8.7162	9.4952	11.0240	7.4951	8.5684	7.9866	8.9992
1.512	7.7047	9.3532	8.9938	10.3102	7.7502	9.1438	8.2568	9.6066
1.606	7.9970	10.0912	8.5954	9.7260	8.0280	9.8031	8.5492	10.2972
1.701	8.3188	10.9249	8.2904	9.2621	8.3251	10.5342	8.8593	11.0555
1.795	8.6670	11.8464	8.0688	8.9095	8.6384	11.3271	9.1833	11.8681
1.890	9.0404	12.8503	7.9209	8.6590	8.9647	12.1733	9.5179	12.7220
1.984	9.4366	13.9316	7.8370	8.5015	9.3006	13.0653	9.8596	13.6053
2.079	9.8534	15.0858	7.8072	8.4278	9.6426	13.9963	10.2051	14.5065
2.173	10.2876	16.3088	7.8218	8.4288	9.9869	14.9601	10.5511	15.4147
2.268	10.7362	17.5970	7.8711	8.4954	10.3298	15.9509	10.8946	16.3200
2.362	11.1958	18.9467	7.9452	8.6184	10.6677	16.9628	11.2327	17.2125
2.457	11.6629	20.3548	8.0356	8.7895	10.9968	17.9896	11.5627	18.0831
2.551	12.1338	21.8189	8.1392	9.0039	11.3138	19.0245	11.8821	18.9227
2.646	12.6051	23.3378	8.2542	9.2576	11.6152	20.0589	12.1888	19.7223
2.740	13.0735	24.9122	8.3787	9.5469	11.8979	21.0818	12.4806	20.4719
2.835	13.5358	26.5466	8.5114	9.8684	12.1588	22.0789	12.7587	21.1605
2.929	13.9892	28.2520	8.6515	10.2195	12.3950	23.0309	13.0149	21.7752
3.024	14.4313	30.0536	8.7983	10.5977	12.6039	23.9134	13.2498	22.2999
3.118	14.8600	32.0115	8.9512	11.0010	12.7834	24.6962	13.4610	22.7142
3.213	15.2738	34.2776	9.1097	11.4277	12.9326	25.3452	13.6453	22.9915
3.307	15.6715	38.0536	9.2736	11.8762	13.0518	25.8244	13.7995	23.0966
3.402	16.0523	20.5421	9.4423	12.3452	13.1441	26.1007	13.9194	22.9823
3.496	16.4159	18.5218	9.6155	12.8336	13.2142	26.1506	14.0060	22.5830
3.590	16.7622	35.1491	9.7929	13.3402	13.2688	25.9688	14.0420	21.8072
3.685	17.0913	38.2312	9.9740	13.8642	13.3141	25.5737	14.0276	20.5245
3.779	17.4038	40.5436	10.1585	14.4047	13.3555	25.0063	13.9570	18.5502
3.874	17.7002	42.6122	10.3459	14.9608	13.3964	24.3209	13.8266	15.6337
3.968	17.9810	44.5759	10.5360	15.5319	13.4386	23.5732	13.6389	11.4712
4.063	18.2471	46.4904	10.7282	16.1172	13.4826	22.8106	13.4100	5.7893
4.157	18.4992	48.3823	10.9222	16.7160	13.5283	22.0680	13.1791	-1.4481
4.252	18.7380	50.2659	11.1177	17.3276	13.5751	21.3678	13.0092	-9.7633
4.346	18.9644	52.1499	11.3141	17.9513	13.6224	20.7222	12.9677	-18.1006
4.441	19.1789	54.0396	11.5112	18.5863	13.6697	20.1360	13.0908	-25.2418

TABLE T16: Static (wavelength independent) polarizability components for the F_2 molecule computed with Hartree-Fock, DFT, CASSCF, CCSD(T) methods. The basis set used in these calculations was *aug-cc-pVQZ*.

	HF		DFT		CASSCF		CCSD(T)	
r	$\alpha_\perp$	$\alpha_\parallel$	$\alpha_\perp$	$\alpha_\parallel$	$\alpha_\perp$	$\alpha_\parallel$	$\alpha_\perp$	$\alpha_\parallel$
1.039	24.9092	50.7139	740.4571	250.0871	24.7330	48.0959	99.3760	357.0977
1.134	14.5791	26.4050	617.4013	227.2737	14.6672	27.5467	42.9059	103.8332
1.228	9.8002	17.5760	509.1774	205.3509	9.7752	17.1710	21.6012	45.8577
1.323	7.3532	11.7012	414.8197	184.3652	7.3663	11.8509	12.8750	24.6221
1.417	6.1450	9.1030	333.3630	164.3630	6.1439	9.0604	9.0344	15.5120
1.512	5.5016	7.5431	263.8417	145.3907	5.5041	7.5589	7.2089	11.1683
1.606	5.1706	6.7813	205.2905	127.4948	5.1712	6.7763	6.2894	8.9464
1.701	5.0092	6.4374	156.7438	110.7216	5.0101	6.4331	5.8177	7.7913
1.795	4.9493	6.4062	117.2363	95.1178	4.9502	6.3915	5.5874	7.2390
1.890	4.9503	6.6079	85.8025	80.7295	4.9517	6.5758	5.4968	7.0706
1.984	4.9887	7.0078	61.4770	67.6034	4.9911	6.9393	5.4913	7.1717
2.079	5.0496	7.5844	43.2943	55.7859	5.0536	7.4440	5.5390	7.4755
2.173	5.1232	8.3251	30.2890	45.3233	5.1297	8.0517	5.6201	7.9366
2.268	5.2032	9.2211	21.4956	36.2621	5.2131	8.7184	5.7215	8.5170
2.362	5.2856	10.2657	15.9488	28.6488	5.2998	9.3950	5.8343	9.1816
2.457	5.3678	11.4528	12.6831	22.5297	5.3874	10.0304	5.9520	9.8953
2.551	5.4486	12.7773	10.7331	17.9514	5.4744	10.5777	6.0702	10.6232
2.646	5.5271	14.2340	9.2942	14.8548	5.5597	11.0002	6.1858	11.3309
2.740	5.6034	15.8181	8.2063	12.7594	5.6427	11.2760	6.2968	11.9856
2.835	5.6774	17.5248	7.4511	11.1718	5.7231	11.3998	6.4017	12.5570
2.929	5.7494	19.3490	6.9347	9.9688	5.8004	11.3810	6.5007	13.0184
3.024	5.8198	21.2855	6.5593	9.1096	5.8742	11.2397	6.5915	13.3479
3.118	5.8888	23.3287	6.2876	8.5121	5.9442	11.0024	6.6750	13.5287
3.213	5.9566	25.4724	6.0979	8.0950	6.0102	10.6969	6.7516	13.5503
3.307	6.0235	27.7101	5.9702	7.8214	6.0718	10.3498	6.8215	13.4103
3.402	6.0893	30.0351	5.8865	7.6662	6.1291	9.9834	6.8853	13.1087
3.496	6.1543	32.4404	5.8370	7.6091	6.1818	9.6157	6.9436	12.6562
3.590	6.2182	34.9187	5.8140	7.6323	6.2302	9.2598	6.9972	12.0678
3.685	6.2810	37.4630	5.8116	7.7241	6.2744	8.9244	7.0469	11.3630
3.779	6.3425	40.0667	5.8249	7.8748	6.3146	8.6149	7.0935	10.5641
3.874	6.4025	42.7232	5.8505	8.0765	6.3511	8.3337	7.1379	9.6949
3.968	6.4609	45.4266	5.8853	8.3224	6.3843	8.0814	7.1806	8.7793
4.063	6.5174	48.1715	5.9273	8.6068	6.4144	7.8571	7.2222	7.8394
4.157	6.5719	50.9532	5.9745	8.9247	6.4419	7.6591	7.2629	6.8951
4.252	6.6242	53.7673	6.0254	9.2717	6.4670	7.4853	7.3029	5.9634
4.346	6.6741	56.6100	6.0789	9.6440	6.4901	7.3332	7.3416	5.0579
4.441	6.7215	59.4783	6.1341	10.0382	6.5115	7.2007	7.3788	4.1890

S4. Determination of accurate potential energy curves using experimental data

A. Motivation

In order to determine the ro-vibrational wave functions with sufficient accuracy using a potential curve ($V(r)$), we first determine parameters for an analytical potential function which yields accurate eigenvalues. For this purpose, we use the developed collocation method with certain initial guess parameters for the chosen analytical potential function. The solutions of the 1-D Schroedinger equation using the chosen potential curve gives us the eigenvalues and the derived transition frequencies, which are then compared with the analogous reference values from experimental datasets. Subsequently, a least-squares non-linear optimization scheme is used to optimize the parameters governing the shape of the potential curve, while minimizing the difference in the computed and reference experimental values of ro-vibrational energies (as well as the transition frequencies).

Several kinds of analytical functions have been used to model the potential energy curves of diatomic molecules. We use the Morse function[48, 49] for HF, DF, HCl, DCl, N_2, $^{14}N^{15}N$, and F_2 molecules which is given by

$$V(r) = \alpha(1 - exp\ \beta)^2 \tag{E22}$$

where $\beta = -c_0\rho + c_1\rho^2 + c_2\rho^3$. For the other molecules, namely, CO and its isotope $^{13}C^{16}O$, we used the Rydberg function[50–52] given by

$$V(r) = -D_e(1 + b\rho)(exp(-b\rho)) + D_e \tag{E23}$$

where $b = \sqrt{\frac{k_e}{D_e}}$. In the above analytical functions, ρ is given by $\rho = r - r_e$.

B. General scheme

We start with first choosing an appropriate analytical function for the studied molecule. We then use some guess initial parameters for the analytical function with a pre-defined vector of internuclear distance (ρ) to generate an initial numerical representation of the potential curve.

We utilize the developed program based on the collocation method with the first guess of the potential function to compute the eigenvalues for the 1-D Schroedinger equation in a time efficient way. In this procedure, Hamiltonian matrices (**H**) for typically four rotational states are constructed with a set of parameter(s) for the potential function (Morse or RKV function). Diagonalization of **H** matrices yields the eigenvalues corresponding to the energies, and eigenvectors corresponding to wave functions, of the involved ro-vibrational states.

Using the sets of computed energies of the states, relevant transition frequencies are then determined. These sets of transition frequencies (and in some cases, the energies of the states) are then compared with the analogous values from accurate high-resolution spectroscopic experiments. The differences were then evaluated as a vector. The square of the Frobenius norm (E) was then computed.

$$E = \sum_i \left(E^{\text{calc.}}_{v,J} - E^{\text{ref.}}_{v,J} \right)^2 + \sum_j \left(\nu^{\text{calc}}_{v,J\rightarrow v',J'} - \nu^{\text{ref.}}_{v,J\rightarrow v',J'} \right)^2 \tag{E24}$$

We then utilize a least-squares non-linear optimization procedure where the numerical value of E is minimized while, the parameters governing the shape of the potential curve are varies.

Eventually, we obtain a set of optimal parameters of the potential function, which gives a minimum difference in comparison to the reference energy levels and transition frequencies.

The reference experimental datasets in our analysis typically covered v =0–3 and J =0–4. For some of the molecules, due to lack of data on the energy levels, only the transition frequencies were used. Specific details about the experimental references for each molecule are given in later tables.

C. Implementation

The above illustrated scheme for the obtaining the potential energy curves for diatomic molecules is implemented in Python using NumPy and SciPy modules. Non-linear optimization in SciPy[53, 54] available

in the module `optimize` is used for minimization of the norm (E) . Specific algorithm used in our analysis was 'Nelder-Mead'[55] with tolerance for convergence set to 1×10^{-9} and number of iterations set to 3000. The methodology of our analysis is pictorially described in Fig. F25. In actual analysis, the vector ρ spanned [0.75, 5.99] bohrs with a step of 0.05 bohrs. Several tests were performed to ensure that a global minimum has been found during the optimization procedure:

1. In this process, several different permutations of initial parameters were tested. In all cases we tried 20–30 sets of initial parameters. The obtained residuals were then checked for their values. Among the tested 20-30 initial sets of parameters, over 80% of the residuals converged to a single value. In some of the cases, the upper limit for the number of iterations were reached.

2. In the next step, we selected the a small subset of initial parameters from the previous test, while looking at the number of iterations required for convergence. The lower number of iterations represent that the initial guess are close to the optimum results. In this second refinement, we added a small magnitude of random noise ($\sim$ 10%) to the set of selected parameters. The optimization process was repeated. In this case, all of the runs converged to the same result.

Individual comparisons of the obtained energy levels and/or transition frequencies after the optimization procedure with the analogous experimental results are shown in Fig. T22–T24 for the studied molecules.

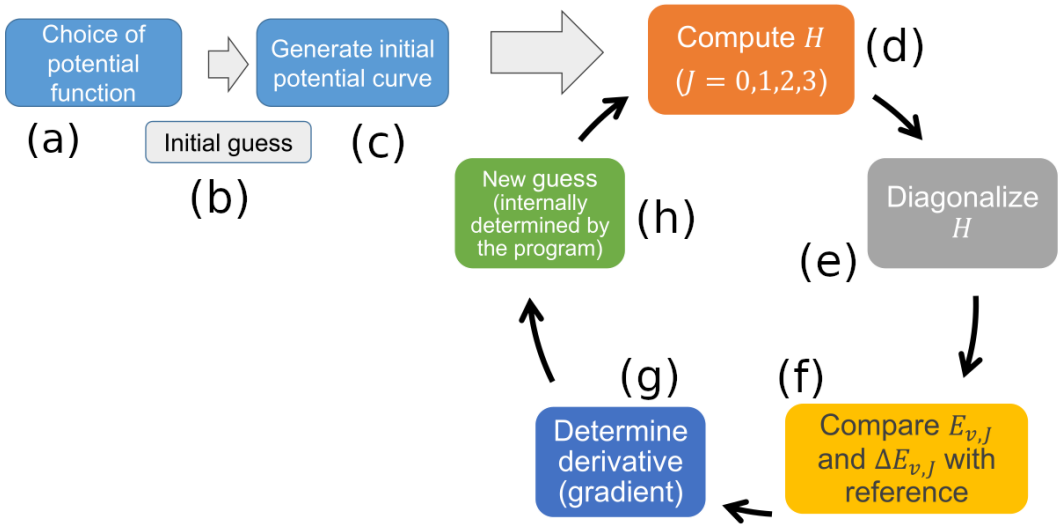

FIG. F25: Overall scheme for the determination of potential energy curve for the studied molecules in this work. We utilize an analytical function (a), and generate an initial curve using guess parameters (b and c). Next, using the guess potential curve, the Hamiltonian matrix is constructed (d), followed by its diagonalization (e). The obtained eigenvalues and transition frequencies are compared to the already prepared reference data-set from literature (f). The sum of the difference is used to obtain the residual. A non-linear optimization procedure is used to minimize the residual while varying the parameters controlling the shape of the potential energy curve (g and h)

D. Results

In this section, the results on the computed transition frequencies (and energies of ro-vibrational states) are compared to the corresponding experimental values. These transitions are among the O-, P-, Q-, R- and/or S- ro-vibrational transitions. The definition of these transitions are shown in Fig.F26.

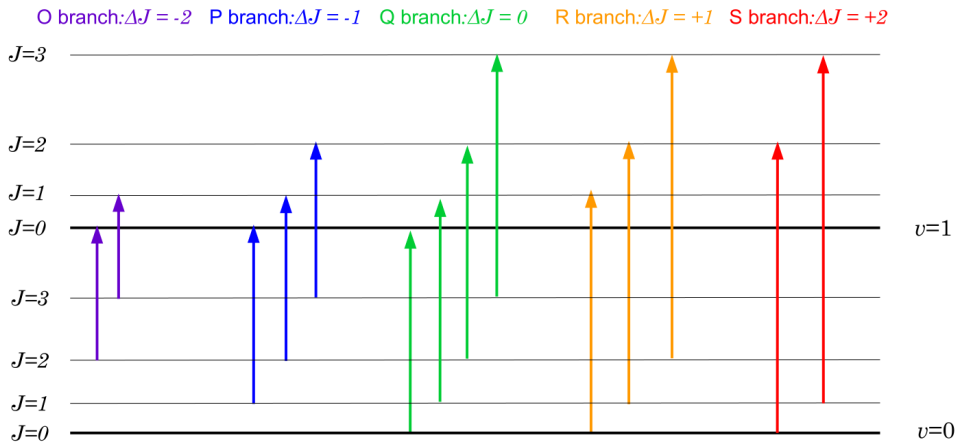

FIG. F26: Illustration showing the different ro-vibrational transitions in molecules. From left to right: O-branch ($\Delta J = -2$) shown in purple, P-branch ($\Delta J = -1$) shown in blue, Q-branch ($\Delta J = 0$) shown in green, R-branch ($\Delta J = +1$) shown in yellow, and S-branch ($\Delta J = +2$) shown in red. The vibrational quantum number may or may not change for the O-, P-, R-, and S- transitions.

TABLE T17: Comparison between the reference values and the calculated results for the ro-vibrational transition frequencies (in cm^{-1}) of HF molecule. The reference values were obtained from the HITRAN database[1] and associated literature.[2–12] A total of 28 transition frequencies spanning $v = 0 - 3$ and $J = 0 - 4$ were used in the present analysis. Ro-vibrational transitions are denoted as : type of transition (P or R) followed by the quantum number of the initial rotational state.

	$v = 0 \rightarrow 0$		
Transition	Expt.	Our	Δ
R0	41.111	41.108	-0.003
R1	82.171	82.165	-0.006
R2	123.129	123.121	-0.008
R3	163.936	163.924	-0.011
	$v = 0 \rightarrow 1$		
	Expt.	Our	Δ
P4	3788.227	3788.569	0.341
P3	3833.661	3833.920	0.259
P2	3877.707	3877.909	0.202
P1	3920.311	3920.484	0.172
R0	4000.989	4001.183	0.194
R1	4038.962	4039.207	0.245
R2	4075.293	4075.615	0.322
R3	4109.935	4110.360	0.424
	$v = 0 \rightarrow 2$		
	Expt.	Our	Δ
P4	7568.575	7568.459	-0.116
P3	7618.519	7618.237	-0.282
P2	7665.573	7665.179	-0.393
P1	7709.682	7709.230	-0.451
R0	7788.855	7788.453	-0.402
R1	7823.819	7823.523	-0.296
R2	7855.641	7855.505	-0.136
R3	7884.278	7884.354	0.075
	$v = 0 \rightarrow 3$		
	Expt.	Our	Δ
P4	11181.781	11182.250	0.468
P3	11236.125	11236.329	0.203
P2	11286.115	11286.140	0.025
P1	11331.693	11331.628	-0.065
R0	11409.397	11409.414	0.017
R1	11442.923	11442.616	-0.307
R2	11468.847	11469.296	0.449
R3	11491.621	11492.415	0.793

TABLE T18: Comparison between the reference values and the calculated results for the ro-vibrational transition frequencies (in cm^{-1}) of DF molecule. The reference values were obtained from the HITRAN database[1] and associated literature.[2–12] A total of 28 transition frequencies spanning $v = 0 - 3$ and $J = 0 - 4$ were used in the present analysis.

	$v = 0 \rightarrow 0$		
Transition	Expt.	Our	Δ
R0	21.718	21.731	0.013
R1	43.423	43.448	0.025
R2	65.099	65.137	0.038
R3	87.733	86.783	-0.949
	$v = 0 \rightarrow 1$		
	Expt.	Our	Δ
P4	2816.374	2816.452	0.077
P3	2839.785	2839.848	0.063
P2	2862.646	2862.704	0.057
P1	2884.943	2885.005	0.061
R0	2927.787	2927.883	0.096
R1	2948.306	2948.433	0.126
R2	2968.206	2968.372	0.166
R3	2987.472	2987.686	0.214
	$v = 0 \rightarrow 2$		
	Expt.	Our	Δ
P4	5628.044	5627.933	-0.110
P3	5653.197	5653.045	-0.152
P2	5677.221	5677.044	-0.176
P1	5700.099	5699.917	-0.182
R0	5742.362	5742.223	-0.138
R1	5761.719	5761.630	-0.088
R2	5779.875	5779.854	-0.021
R3	5796.818	5796.883	0.064
	$v = 0 \rightarrow 3$		
	Expt.	Our	Δ
P4	8350.156	8350.202	0.045
P3	8377.021	8376.992	-0.028
P2	8402.186	8402.112	-0.074
P1	8425.635	8425.544	-0.090
R0	8467.327	8467.291	-0.035
R1	8485.542	8485.577	0.035
R2	8501.987	8502.122	0.134
R3	8516.651	8516.913	0.262

TABLE T19: Comparison between the reference values and the calculated results for the ro-vibrational transition frequencies (in cm^{-1}) of HCl molecule. The reference values were obtained from the HITRAN database[1] and associated literature.[2, 13–22] A total of 28 transition frequencies spanning $v = 0 - 3$ and $J = 0 - 4$ were used in the present analysis.

	$v = 0 \rightarrow 0$		
Transition	Expt.	Our	Δ
R0	20.878	20.840	-0.037
R1	41.743	41.668	-0.075
R2	62.584	62.470	-0.113
R3	83.386	83.235	-0.151
	$v = 0 \rightarrow 1$		
	Expt.	Our	Δ
P4	2798.942	2799.124	0.182
P3	2821.586	2821.535	-0.033
P2	2843.624	2843.435	-0.188
P1	2865.098	2864.812	-0.286
R0	2906.246	2905.944	-0.302
R1	2925.896	2925.674	-0.221
R2	2944.913	2944.830	-0.082
R3	2963.285	2963.399	0.114
	$v = 0 \rightarrow 2$		
	Expt.	Our	Δ
P4	5577.331	5577.856	0.525
P3	5601.765	5601.929	0.164
P2	5625.027	5624.938	-0.089
P1	5647.104	5646.868	-0.236
R0	5687.650	5687.446	-0.203
R1	5706.093	5706.068	-0.025
R2	5723.301	5723.562	0.260
R3	5739.262	5739.914	0.652
	$v = 0 \rightarrow 3$		
	Expt.	Our	Δ
P4	8252.528	8252.958	0.430
P3	8278.760	8278.710	-0.050
P2	8303.222	8302.838	-0.384
P1	8325.898	8325.328	-0.570
R0	8365.844	8365.346	-0.497
R1	8383.089	8382.849	-0.239
R2	8398.498	8398.664	0.165
R3	8412.062	8412.778	0.715

TABLE T20: Comparison between the reference values and the calculated results for the ro-vibrational transition frequencies (in cm^{-1}) of DCl molecule. The reference values were obtained from the HITRAN database[1] and associated literature.[2, 4, 14, 16, 17, 21, 23, 24] A total of 28 transition frequencies spanning $v = 0 - 3$ and $J = 0 - 4$ were used in the present analysis.

	$v = 0 \rightarrow 0$		
Transition	Expt.	Our	Δ
R0	10.784	10.768	-0.015
R1	21.564	21.533	-0.030
R2	32.338	32.292	-0.045
R3	43.102	43.041	-0.061
	$v = 0 \rightarrow 1$		
	Expt.	Our	Δ
P4	2046.607	2046.670	0.062
P3	2058.046	2058.027	-0.018
P2	2069.269	2069.191	-0.077
P1	2080.275	2080.159	-0.115
R0	2101.618	2101.494	-0.123
R1	2111.949	2111.853	-0.095
R2	2122.048	2122.003	-0.044
R3	2131.913	2131.940	0.027
	$v = 0 \rightarrow 2$		
	Expt.	Our	Δ
P4	4082.639	4082.849	0.209
P3	4094.747	4094.819	0.071
P2	4106.418	4106.391	-0.026
P1	4117.647	4117.564	-0.082
R0	4138.766	4138.694	-0.072
R1	4148.650	4148.645	-0.005
R2	4158.080	4158.182	0.102
R3	4167.051	4167.302	0.251
	$v = 0 \rightarrow 3$		
	Expt.	Our	Δ
P4	6065.324	6065.494	0.169
P3	6078.099	6078.081	-0.018
P2	6090.214	6090.065	-0.149
P1	6101.665	6101.443	-0.222
R0	6122.563	6122.368	-0.195
R1	6132.003	6131.907	-0.095
R2	6140.765	6140.828	0.062
R3	6148.848	6149.125	0.277

TABLE T21: Comparison between the reference values and the calculated results for the ro-vibrational transition frequencies (in cm^{-1}) of CO molecule. The reference values were obtained from the HITRAN database[1] and associated literature.[25–36] A total of 24 transition frequencies and 20 energy levels (in Table T22) spanning $v = 0 - 3$ and $J = 0 - 4$ were used in the present analysis.

	$v = 0 \rightarrow 1$		
Transition	Expt.	Our	Δ
P4	2127.682	2127.545	-0.136
P3	2131.631	2131.490	-0.140
P2	2135.546	2135.403	-0.142
P1	2139.426	2139.284	-0.141
R0	2146.081	2146.950	0.869
R1	2150.856	2150.734	-0.121
R2	2154.595	2154.485	-0.109
R3	2158.299	2158.203	-0.095

	$v = 0 \rightarrow 2$		
	Expt.	Our	Δ
P4	4244.263	4244.179	-0.083
P3	4247.385	4248.222	0.837
P2	4252.302	4252.201	-0.100
P1	4256.217	4256.115	-0.101
R0	4263.837	4263.748	-0.088
R1	4267.542	4267.466	-0.075
R2	4270.781	4271.119	0.338
R3	4274.740	4274.707	-0.032

	$v = 0 \rightarrow 3$		
	Expt.	Our	Δ
P4	6334.430	6333.430	0.000
P3	6338.589	6338.571	-0.017
P2	6342.644	6342.615	-0.028
P1	6346.594	6346.562	-0.031
R0	6354.179	6354.162	-0.016
R1	6357.813	6357.815	0.022
R2	6361.343	6361.370	0.027
R3	6364.767	6364.826	0.059

TABLE T22: Comparison of the calculated energy levels of CO with corresponding reference data[37] in the ground electronic state.

	$v = 0$		
Level	Expt.	Our	Δ
$v = 0, J = 0$	0	0	0
$v = 0, J = 1$	3.845	3.848	0.003
$v = 0, J = 2$	11.535	11.546	0.011
$v = 0, J = 3$	23.069	23.092	0.022
$v = 0, J = 4$	38.448	38.486	0.038
	$v = 1$		
	Expt.	Our	Δ
$v = 1, J = 0$	2143.271	2143.138	-0.137
$v = 1, J = 1$	2147.081	2146.950	-0.130
$v = 1, J = 2$	2154.701	2154.582	-0.118
$v = 1, J = 3$	2166.130	2166.031	-0.098
$v = 1, J = 4$	2181.369	2181.295	-0.073
	$v = 2$		
	Expt.	Our	Δ
$v = 1, J = 0$	4260.062	4259.964	-0.137
$v = 1, J = 1$	4263.837	4263.748	-0.130
$v = 1, J = 2$	4271.387	4271.315	-0.118
$v = 1, J = 3$	4282.712	4282.666	-0.098
$v = 1, J = 4$	4297.810	4297.799	-0.073
	$v = 3$		
	Expt.	Our	Δ
$v = 2, J = 0$	6350.439	6350.411	-0.027
$v = 2, J = 1$	6354.179	6354.162	-0.016
$v = 2, J = 2$	6361.659	6361.664	0.005
$v = 2, J = 3$	6372.878	6372.916	0.038
$v = 2, J = 4$	6387.837	6387.918	0.081
	$v = 4$		
	Expt.	Our	Δ
$v = 3, J = 0$	8414.469	8414.396	-0.072
$v = 3, J = 1$	8418.174	8418.114	-0.059
$v = 3, J = 2$	8425.584	8425.550	-0.034
$v = 3, J = 3$	8436.699	8436.704	0.055
$v = 3, J = 4$	8451.517	8451.574	0.057

TABLE T23: Comparison between the reference values and the calculated results for the ro-vibrational transition frequencies (in cm^{-1}) of $^{13}C^{16}O$ molecule. The reference values were obtained from the HITRAN database[1] and associated literature.[25–28, 31, 33–36, 38] A total of 24 transition frequencies and 20 energy levels (in Table T22) spanning $v = 0 - 3$ and $J = 0 - 4$ were used in the present analysis.

	$v = 0 \rightarrow 0$		
Transition	Expt.	Our	Δ
R0	3.675	3.674	-0.001
R1	7.351	7.348	-0.003
R2	11.027	11.021	-0.006
R3	14.702	14.695	-0.007
	$v = 0 \rightarrow 1$		
	Expt.	Our	Δ
P4	2081.168	2081.159	-0.009
P3	2084.941	2084.923	-0.018
P2	2088.682	2088.657	-0.024
P1	2092.390	2092.362	-0.028
R0	2099.710	2099.680	-0.029
R1	2103.320	2103.293	-0.027
R2	2106.897	2106.875	-0.021
R3	2110.442	2110.427	-0.014
	$v = 0 \rightarrow 2$		
	Expt.	Our	Δ
P4	4151.724	4151.763	0.039
P3	4155.595	4155.619	0.024
P2	4159.401	4159.415	0.013
P1	4163.143	4163.150	0.007
R0	4170.429	4170.437	0.012
R1	4173.974	4173.989	0.015
R2	4177.453	4177.480	0.027
R3	4180.876	4180.910	0.034
	$v = 0 \rightarrow 3$		
	Expt.	Our	Δ
P4	6197.026	6197.041	0.014
P3	6200.996	6200.989	-0.006
P2	6204.868	6204.846	-0.021
P1	6208.642	6208.612	-0.030
R0	6215.895	6215.868	-0.027
R1	6219.375	6219.359	-0.015
R2	6222.756	6222.758	0.001
R3	6226.039	6226.065	0.026

TABLE T24: Comparison between the reference values and the calculated results for the ro-vibrational transition frequencies (in cm^{-1}) of N_2 molecule. The reference values were obtained from the HITRAN database[1] and associated literature.[39–41] A total of 33 transition frequencies spanning $v = 0 - 3$ and $J = 0 - 4$ were used in the present analysis.

	$v = 0 \rightarrow 0$		
Transition	Expt.	Our	Δ
S0	11.937	11.935	-0.002
S1	19.895	19.892	-0.003
S2	27.852	27.848	-0.004
	$v = 0 \rightarrow 1$		
	Expt.	Our	Δ
O4	2301.955	2301.959	0.004
O3	2309.981	2309.984	0.003
O2	2317.974	2317.975	0.001
Q1	2329.876	2329.876	0.000
Q2	2329.807	2329.808	0.001
Q3	2329.703	2329.706	0.003
Q4	2329.564	2329.569	0.005
S0	2341.744	2341.744	0.000
S1	2349.598	2349.598	0.000
S2	2357.416	2357.418	0.002
	$v = 0 \rightarrow 2$		
	Expt.	Our	Δ
O4	4603.105	4603.105	0.000
O3	4611.201	4611.198	-0.003
O2	4619.228	4619.223	-0.005
Q1	4631.096	4631.090	-0.006
Q2	4630.957	4630.953	-0.004
Q3	4630.748	4630.748	0.000
Q4	4630.470	4630.475	0.005
S0	4642.894	4642.889	-0.005
S1	4650.643	4650.641	-0.002
S2	4658.322	4658.323	0.001
	$v = 0 \rightarrow 3$		
	Expt.	Our	Δ
O4	6875.556	6875.558	0.002
O3	6883.722	6883.719	-0.003
O2	6891.784	6891.779	-0.005
Q1	6903.617	6903.612	-0.005
Q2	6903.408	6903.406	-0.002
Q3	6903.095	6903.098	0.003
Q4	6902.676	6902.687	0.011
S0	6915.346	6915.342	-0.004
S1	6922.990	6922.991	0.001
S2	6930.529	6930.536	0.007

TABLE T25: Comparison between the reference values and the calculated results for the ro-vibrational transition frequencies (in cm^{-1}) of $^{14}N^{15}N$ molecule. The reference values were obtained from the HITRAN database[1] and associated literature.[39–41] A total of 13 transition frequencies spanning v =0–1 and J =0–4 were used in the present analysis.

	$v = 0 \rightarrow 0$		
Transition	Expt.	Our	Δ
S0	11.541	11.529	-0.011
S1	19.235	19.215	-0.019
S2	26.928	26.900	-0.027
	$v = 0 \rightarrow 1$		
	Expt.	Our	Δ
O4	2264.312	2264.324	0.011
O3	2272.072	2272.051	-0.020
O2	2279.799	2279.758	-0.040
Q1	2291.010	2291.267	0.256
Q2	2291.142	2291.224	0.082
Q3	2291.241	2291.161	-0.080
Q4	2291.307	2291.076	-0.231
S0	2302.782	2302.754	-0.028
S1	2310.377	2310.376	-0.001
S2	2317.938	2317.976	0.038

TABLE T26: Comparison between the calculated and reference datasets of ro-vibrational transition frequencies in the F_2 molecule.[42, 43] A total of 13 transition frequencies spanning v =0–1 and J =3–11 were used in the present analysis.

	$v = 0 \rightarrow 0$		
Transition	Expt.	Our	Δ
S5	22.966	22.961	-0.005
S7	30.016	30.019	0.003
S9	37.071	37.072	0.001
	$v = 0 \rightarrow 1$		
	Expt.	Our	Δ
O11	855.719	855.655	-0.064
O9	863.212	863.183	-0.029
O7	870.604	870.604	0.000
Q5	893.553	893.565	0.012
Q7	893.217	893.202	-0.015
Q9	892.777	892.727	-0.005
Q11	892.231	892.139	-0.092
S5	916.169	916.163	-0.005
S7	922.782	922.746	-0.036
S9	929.286	929.211	-0.075

TABLE T27: Comparison between the calculated and reference datasets of vibration energy levels in the F_2 molecule.[44]

Transition	Expt.	Our	Δ
$v = 0 \rightarrow 1$	893.00	893.98	0.98
$v = 0 \rightarrow 2$	1764.15	1763.94	-0.21
$v = 0 \rightarrow 3$	2610.22	2609.86	-0.35
$v = 0 \rightarrow 4$	3431.53	3431.74	0.22

E. Harmonic wave functions

TABLE T28: Molecular parameters used for generating the harmonic potential energy curves for the studied molecules

Molecule	ω_e (cm^{-1})	r_e (Å)	**Reference**
H_2	4401.2100	0.741440	Ref. [56]
HD	3813.1000	0.741420	Ref. [56]
D_2	3115.5000	0.741520	Ref. [56]
HF	4138.3200	0.916800	Ref. [56]
DF	2998.1900	0.916940	Ref. [56]
HCl	2990.9460	1.274550	Ref. [56]
DCl	2145.1630	1.274581	Ref. [56]
CO	2169.8136	1.1283	Ref. [56]
$^{13}C^{16}O$	2121.4395	1.1283	Ref. [57]
N_2	2358.5849	1.097680	Ref. [56]
$^{14}N^{15}N$	2319.0679	1.097680	Ref. [58]
F_2	916.6400	1.411930	Ref. [56]

TABLE T29: Energy levels obtained using the harmonic wave functions for the 12 diatomic molecules studied in this work.

	H_2		HD		D_2	
	Levels	**Intervals**	**Levels**	**Intervals**	**Levels**	**Intervals**
0	2200.6050		1906.5500		1557.7500	
1	6601.8150	4401.2100	5719.6500	3813.1000	4673.2500	3115.5000
2	11003.0249	4401.2100	9532.7499	3813.0999	7788.7499	3115.4999
3	15404.2353	4401.2104	13345.8497	3813.0998	10904.2496	3115.4998
4	19805.4509	4401.2156	17158.9496	3813.0999	14019.7493	3115.4996
5	24206.7087	4401.2578	20972.0512	3813.1015	17135.2487	3115.4994
6	28608.2316	4401.5229	24785.1663	3813.1151	20250.7480	3115.4993

	HF		DF		HCl	
	Levels	**Intervals**	**Levels**	**Intervals**	**Levels**	**Intervals**
0	2069.1600		1499.0950		1495.4730	
1	6207.4799	4138.3199	4497.2849	2998.1899	4486.4190	2990.9460
2	10345.7997	4138.3198	7495.4746	2998.1897	7477.3649	2990.9459
3	14484.1192	4138.3195	10493.6640	2998.1894	10468.3107	2990.9458
4	18622.4385	4138.3192	13491.8529	2998.1889	13459.2564	2990.9457
5	22760.7572	4138.3188	16490.0412	2998.1883	16450.2019	2990.9455
6	26899.0755	4138.3183	19488.2288	2998.1876	19441.1472	2990.9453

	DCl		CO		$^{13}C^{16}O$	
	Levels	**Intervals**	**Levels**	**Intervals**	**Levels**	**Intervals**
0	1072.5815		1084.9067		1060.7197	
1	3217.7445	2145.1630	3254.7198	2169.8131	3182.1586	2121.4390
2	5362.9073	2145.1629	5424.5317	2169.8120	5303.5965	2121.4379
3	7508.0701	2145.1627	7594.3420	2169.8102	7425.0326	2121.4361
4	9653.2327	2145.1626	9764.1497	2169.8078	9546.4661	2121.4335
5	11798.3950	2145.1623	11933.9543	2169.8046	11667.8964	2121.4303
6	13943.5570	2145.1620	14103.7550	2169.8007	13789.3228	2121.4263

	N_2		$^{14}N^{15}N$		F_2	
	Levels	**Intervals**	**Levels**	**Intervals**	**Levels**	**Intervals**
0	1179.2923		1159.5338		458.3200	
1	3537.8765	2358.5842	3478.6010	2319.0672	1374.9599	916.6399
2	5896.4593	2358.5828	5797.6667	2319.0657	2291.5997	916.6398
3	8255.0397	2358.5804	8116.7301	2319.0633	3208.2392	916.6395
4	10613.6168	2358.5771	10435.7901	2319.0600	4124.8784	916.6392
5	12972.1897	2358.5729	12754.8457	2319.0557	5041.5170	916.6387
6	15330.7573	2358.5677	15073.8961	2319.0504	5958.1552	916.6381

S5. Solution of the 1-D radial nuclear equation

A. Introduction

Energies of the ro-vibrational system and corresponding wave functions can be obtained by a numerical solution to following equation

$$\left(\frac{-1}{2\mu r^2}\frac{\partial}{\partial r}r^2\frac{\partial}{\partial r}+\frac{J(J+1)}{2\mu r^2}+V(r)\right)\psi_{v,J}=E_{v,J}\psi_{v,J} \tag{E25}$$

where the first term is kinetic energy, the second term is centrifugal term, and the third term is potential energy. The kinetic term of diatomic molecule can be expressed as

$$\frac{-1}{\mu r}\frac{\partial}{\partial r}-\frac{1}{2\mu}\frac{\partial^2}{\partial r^2} \tag{E26}$$

In order to solve the numerical solution of Eqn. (E25), we applied the five point stencil. Stencil is often used to solve the numerical solution of partial differential equations. In numerical analysis, given a one-dimensional or two-dimensional square grid, the five point stencil in the grid consists of the point and other four points adjacent to it. It describes a finite difference approximation of the derivative at the grid points.

1. *Procedure*

The collocation method for obtaining numerical solutions to differential equations is based on using the appropriate differences on a grid of points rather than continuous derivatives. In this method, truncated Taylor series expansions at each grid point are used to effectively compute numerical derivatives. For a function $f(x)$, the central difference expression of up to the the 5^{th}-order derivative can be derived by the Taylor series expansion at five grid points $f(x-2h)$, $f(x-h)$, $f(x)$, $f(x+h)$ and $f(x+2h)$:

$$\begin{aligned}
f(x-2h) &= f(x)-2hf^{(1)}(x)+\frac{4h^2f^{(2)}(x)}{2!}-\frac{8h^3f^{(3)}(x)}{3!}+\frac{16h^4f^{(4)}(x)}{4!}-\frac{32h^5f^{(5)}(x)}{5!}\\
f(x-h) &= f(x)-hf^{(1)}(x)+\frac{h^2f^{(2)}(x)}{2!}-\frac{h^3f^{(3)}(x)}{3!}+\frac{h^4f^{(4)}(x)}{4!}-\frac{h^5f^{(5)}(x)}{5!}\\
f(x) &= f(x)+0+0+0+0+0\\
f(x+h) &= f(x)+hf^{(1)}(x)+\frac{h^2f^{(2)}(x)}{2!}+\frac{h^3f^{(3)}(x)}{3!}+\frac{h^4f^{(4)}(x)}{4!}+\frac{h^5f^{(5)}(x)}{5!}\\
f(x+2h) &= f(x)+2hf^{(1)}(x)+\frac{4h^2f^{(2)}(x)}{2!}+\frac{8h^3f^{(3)}(x)}{3!}+\frac{16h^4f^{(4)}(x)}{4!}+\frac{32h^5f^{(5)}(x)}{5!},
\end{aligned} \tag{E27}$$

To obtain the numerical solution of first derivative, taking difference between the first equation and the last equation in Eqn. E27 gives

$$f(x+2h)-f(x-2h)=4hf^{(1)}(x)+\frac{16h^3f^{(3)}(x)}{3!}+\frac{64h^5f^{(5)}(x)}{5!}. \tag{E28}$$

The difference between the second equation and the last second equation in Eqn. E27 gives

$$f(x+h)-f(x-h)=2hf^{(1)}(x)+\frac{2h^3f^{(3)}(x)}{3!}+\frac{2h^5f^{(5)}(x)}{5!}. \tag{E29}$$

Subtracting Eqn. E28 to eight times of Eqn. E29

$$-f(x+2h)+8f(x+h)-8f(x-h)+f(x-2h)=12hf^{(1)}+\frac{48h^5f^{(5)}(x)}{5!}, \tag{E30}$$

where the first derivative is obtained. Here we have truncated up to the the 4^{th} derivative term, and the last term consisting of 5^{th} derivative term is the error estimation in this approximation. Rearranging the Eqn. E30, we obtain the first derivative as a function of $f(x)$ at the five grid points

$$
\begin{aligned}
f^{(1)} =& C_0 f(x-2h) + C_1 f(x-h) + C_2 f(x) + C_3 f(x+h) \\
&+ C_4 f(x+2h) + \text{error}(h) \\
=& \frac{f(x-2h) - 8f(x-h) + 8f(x+h) - f(x+2h)}{12h} + \frac{h^4 f^{(5)}(x)}{30}.
\end{aligned} \tag{E31}
$$

The coefficients of each grid points for the first derivative is ($\frac{1}{12h}$,$\frac{-8}{12h}$,0,$\frac{8}{12h}$,$\frac{-1}{12h}$). The last term, $\frac{h^4 f^{(5)}(x)}{30}$, is the truncation error. The truncation error is step size (h) dependent, and is generalized as

$$
\text{error}(h^n) = \frac{h^n f^{(n+1)}(x)}{(n+1)(n+2)}. \tag{E32}
$$

The process of obtaining the coefficients relevant to a particular derivative can also be thought of as a set of linear equations that easily solvable using matrix equation. For the center difference Eqn. E31 is truncated at the 4^{th}-order derivative,

$$
\begin{aligned}
f(x-2h) &= f(x) - 2hf^{(1)}(x) + \frac{4h^2 f^{(2)}(x)}{2!} - \frac{8h^3 f^{(3)}(x)}{3!} + \frac{16h^4 f^{(4)}(x)}{4!} \\
f(x-h) &= f(x) - hf^{(1)}(x) + \frac{h^2 f^{(2)}(x)}{2!} - \frac{h^3 f^{(3)}(x)}{3!} + \frac{h^4 f^{(4)}(x)}{4!} \\
f(x) &= f(x) + 0 + 0 + 0 + 0 \\
f(x+h) &= f(x) + hf^{(1)}(x) + \frac{h^2 f^{(2)}(x)}{2!} + \frac{h^3 f^{(3)}(x)}{3!} + \frac{h^4 f^{(4)}(x)}{4!} \\
f(x+2h) &= f(x) + 2hf^{(1)}(x) + \frac{4h^2 f^{(2)}(x)}{2!} + \frac{8h^3 f^{(3)}(x)}{3!} + \frac{16h^4 f^{(4)}(x)}{4!},
\end{aligned} \tag{E33}
$$

which the linear equations Eqn. E33 can be transformed into a matrix (A) where the value of each element are the values of Taylor series coefficients

$$
A = \begin{bmatrix}
1 & 1 & 1 & 1 & 1 \\
-2 & -1 & 0 & 1 & 2 \\
2 & \frac{1}{2} & 0 & \frac{1}{2} & 2 \\
\frac{-8}{6} & \frac{-1}{6} & 0 & \frac{1}{6} & \frac{8}{6} \\
\frac{16}{24} & \frac{1}{24} & 0 & \frac{1}{24} & \frac{16}{24}
\end{bmatrix}. \tag{E34}
$$

We can use matrix (A) to build up matrix equation $AC = B$

$$
[A]_{5*5}[C]_{5*1} = [B]_{5*1} \tag{E35}
$$

$$
\begin{bmatrix}
1 & 1 & 1 & 1 & 1 \\
-2 & -1 & 0 & 1 & 2 \\
2 & \frac{1}{2} & 0 & \frac{1}{2} & 2 \\
\frac{-8}{6} & \frac{-1}{6} & 0 & \frac{1}{6} & \frac{8}{6} \\
\frac{16}{24} & \frac{1}{24} & 0 & \frac{1}{24} & \frac{16}{24}
\end{bmatrix}
\begin{bmatrix} C_0 \\ C_1 \\ C_2 \\ C_3 \\ C_4 \end{bmatrix}
=
\begin{bmatrix} f^{(0)} \\ f^{(1)} \\ f^{(2)} \\ f^{(3)} \\ f^{(4)} \end{bmatrix}. \tag{E36}
$$

Using the matrix equation (E36) the coefficients (C_0,C_1,C_2,C_3 and C_4) can be obtained by assign the number of column matrix B. The below conditions are for the first derivative and the second derivative

$$
\begin{bmatrix} 0 \\ 1 \\ 0 \\ 0 \\ 0 \end{bmatrix} \text{ for the first derivative, and } \begin{bmatrix} 0 \\ 0 \\ 1 \\ 0 \\ 0 \end{bmatrix} \text{ for the second derivative.} \tag{E37}
$$

Matrix equation $AC = B$ can be solved by $C = A^{-1}B$, when the A is invertible. Each set of coefficients has to be further divided with the value of h^n for the n^{th}-order derivative

$$C : (\frac{C_0}{h}, \frac{C_1}{h}, \frac{C_2}{h}, \frac{C_3}{h}, \frac{C_4}{h}) \text{ for the first derivative, and} \tag{E38}$$

$$C : (\frac{C_0}{h^2}, \frac{C_1}{h^2}, \frac{C_2}{h^2}, \frac{C_3}{h^2}, \frac{C_4}{h^2}) \text{ for the second derivative.} \tag{E39}$$

2. *Hamiltonian matrix*

To build up the Hamiltonian matrix for the n-points potential curve, the similar procedure can be used to calculate the forward and backward difference methods. For the first grid point x_0, the deviation can be describe using forward difference, using expansions over $f(x_0)$,$f(x_0 + h)$,$f(x_0 + 2h)$,$f(x_0 + 3h)$, and $f(x_1 + 4h)$. For the second point x_1, the asymmetric derivative can be employed, using expansions over $f(x_1 - h)$,$f(x_1)$,$f(x_1 + h)$,$f(x_1 + 2h)$, and $f(x_1 + 3h)$. From the third point to $(n-2)^{\text{th}}$ point, the symmetric derivative are employed, using expansions over $f(x_k - 2h)$,$f(x_k - h)$,$f(x_k)$,$f(x_k + h)$, and $f(x_k + 2h)$. For the last second point x_{n-1}, the asymmetric derivative similar to x_1 can be used, taking expansion of $f(x_{n-1} - 3h)$,$f(x_{n-1} - 2h)$,$f(x_{n-1} - h)$,$f(x_{n-1})$, and $f(x_{n-1} + h)$. For the last point the backward derivative can be employed, taking expansion of $f(x_n - 4h)$,$f(x_n - 3h)$,$f(x_n - 2h)$,$f(x_n - h)$, and $f(x_n)$.

The first derivative term of Eqn. E26 can be expressed as first derivative matrix ($\mathbb{F}$) using coefficients of each grid points and step h

$$\mathbb{F} = \begin{bmatrix} C_0^{x_0}/h & C_1^{x_0+h}/h & C_2^{x_0+2h}/h & C_3^{x_0+3h}/h & C_4^{x_0+4h}/h \\ C_0^{x_1-h}/h & C_1^{x_1}/h & C_2^{x_1+h}/h & C_3^{x_1+2h}/h & C_4^{x_1+3h}/h \\ C_0^{x_2-2h}/h & C_1^{x_2-h}/h & C_2^{x_2}/h & C_3^{x_2+h}/h & C_4^{x_2+2h}/h \\ \vdots & \vdots & \vdots & \vdots & \vdots \\ C_0^{x_{n-2}-2h}/h & C_1^{x_{n-2}-h}/h & C_2^{x_{n-2}}/h & C_3^{x_{n-2}+h}/h & C_4^{x_{n-2}+2h}/h \\ C_0^{x_{n-1}-3h}/h & C_1^{x_{n-1}-2h}/h & C_2^{x_{n-1}-h}/h & C_3^{x_{n-1}}/h & C_4^{x_{n-1}+h}/h \\ C_0^{x_n-4h}/h & C_1^{x_n-3h}/h & C_2^{x_n-2h}/h & C_3^{x_n-h}/h & C_4^{x_{n+1}}/h \end{bmatrix}. \tag{E40}$$

Similarly, the second derivative term of Eqn. E26 can be written as second derivative matrix($\mathbb{S}$) using coefficients of each grid points and the value h^2

$$\mathbb{S} = \begin{bmatrix} C_0^{x_0}/h^2 & C_1^{x_0+h}/h^2 & C_2^{x_0+2h}/h^2 & C_3^{x_0+3h}/h^2 & C_4^{x_0+4h}/h^2 \\ C_0^{x_1-h}/h^2 & C_1^{x_1}/h^2 & C_2^{x_1+h}/h^2 & C_3^{x_1+2h}/h^2 & C_4^{x_1+3h}/h^2 \\ C_0^{x_2-2h}/h^2 & C_1^{x_2-h}/h^2 & C_2^{x_2}/h^2 & C_3^{x_2+h}/h^2 & C_4^{x_2+2h}/h^2 \\ \vdots & \vdots & \vdots & \vdots & \vdots \\ C_0^{x_{n-2}-2h}/h^2 & C_1^{x_{n-2}-h}/h^2 & C_2^{x_{n-2}}/h^2 & C_3^{x_{n-2}+h}/h^2 & C_4^{x_{n-2}+2h}/h^2 \\ C_0^{x_{n-1}-3h}/h^2 & C_1^{x_{n-1}-2h}/h^2 & C_2^{x_{n-1}-h}/h^2 & C_3^{x_{n-1}}/h^2 & C_4^{x_{n-1}+h}/h^2 \\ C_0^{x_n-4h}/h^2 & C_1^{x_n-3h}/h^2 & C_2^{x_n-2h}/h^2 & C_3^{x_n-h}/h^2 & C_4^{x_{n+1}}/h^2 \end{bmatrix}. \tag{E41}$$

In $\mathbb{F}$ and $\mathbb{S}$ matrices, each grid point takes five columns, and the first and last two points use asymmetric derivatives, while other points use symmetric derivative. We can assign each grid point and the corresponding values into the Hamiltonian matrix (**H**). The **H** is a square matrix, the row is related to each grid point (e.g. first row is corresponding to x_0, second row is corresponding to x_1), and the column is related to the values for Taylor series expansion. Similar to $\mathbb{F}$ and $\mathbb{S}$, each point occupies five columns, but the difference is that the position of the value in **H** should be considered. For example, the first grid point x_0 using expansion over $f(x_0)$, $f(x_0 + h)$, $f(x_0 + 2h)$, $f(x_0 + 3h)$, $f(x_0 + 4h)$, it use the same value of $f(x_0)$, $f(x_1)$, $f(x_2)$, $f(x_3)$, $f(x_4)$. The first grid point occupies the first column to the fifth column. The second grid point x_1 using expansion over $f(x_1 - h)$, $f(x_1)$, $f(x_1 + h)$, $f(x_1 + 2h)$, $f(x_1 + 3h)$, the value of $f(x_0)$, $f(x_1)$, $f(x_2)$, $f(x_3)$, $f(x_4)$ are used. Analogous to the first grid point x_0, x_1 occupies the first five columns. Other grid points

Point on gird	Taylor expansion required						
x_0	x_0	x_0+h	x_0+2h	x_0+3h	x_0+4h	Forward	asymmetric
x_1	x_1-h	x_1	x_1+h	x_1+2h	x_0+3h	Forward	asymmetric
x_2	x_2-2h	x_2-h	x_2	x_2+h	x_2+2h	Central	symmetric
⋮	⋮	⋮	⋮	⋮	⋮	Central	symmetric
x_{n-2}	$x_{n-2}-2h$	$x_{n-2}-h$	x_{n-2}	$x_{n-2}+h$	$x_{n-2}+2h$	Central	symmetric
x_{n-1}	$x_{n-1}-3h$	$x_{n-1}-2h$	$x_{n-1}-h$	x_{n-1}	$x_{n-1}+h$	Backward	asymmetric
x_n	$x_{n-2}-2h$	$x_{n-2}-h$	x_{n-2}	$x_{n-2}+h$	$x_{n-2}+2h$	Backward	asymmetric

FIG. F27: The Taylor expansions required to obtain the derivatives at a specific point on the grid, and their corresponding characteristic from point x_0 to x_n with step of h.

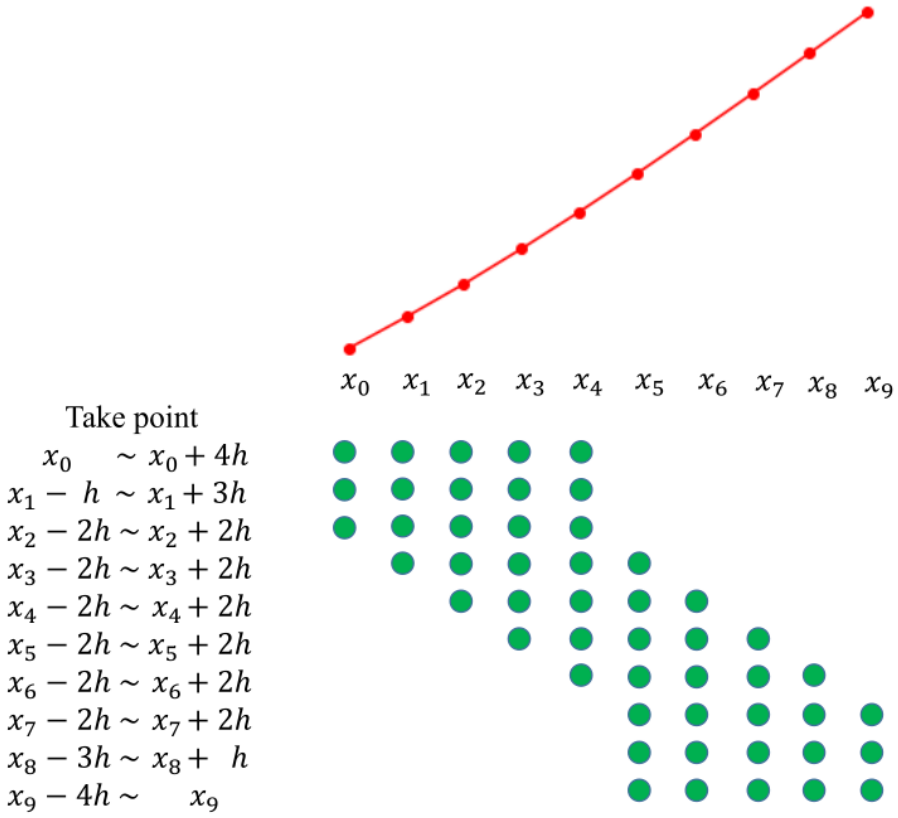

FIG. F28: Ten points ($x_0 \sim x_9$) example for the location of each grid point and corresponding values are used shown in green dots.

and their occupied positions in **H** shown in the Fig. F29. The first-derivative and second-derivative term of ro-vibrational system are filled into **H** using the coefficient of $\mathbb{F}$ and $\mathbb{S}$ shown in green and blue region of Fig. F29. The non-derivative term $k(x)$ contains the rotational part and vibrational part

$$k(x) = \frac{J(J+1)}{2\mu x^2} + V(x), \tag{E42}$$

$k(x)$, namely the centrifugal term and potential energy term, are added on the diagonal of **H**, shown in blue region in Fig. F29.

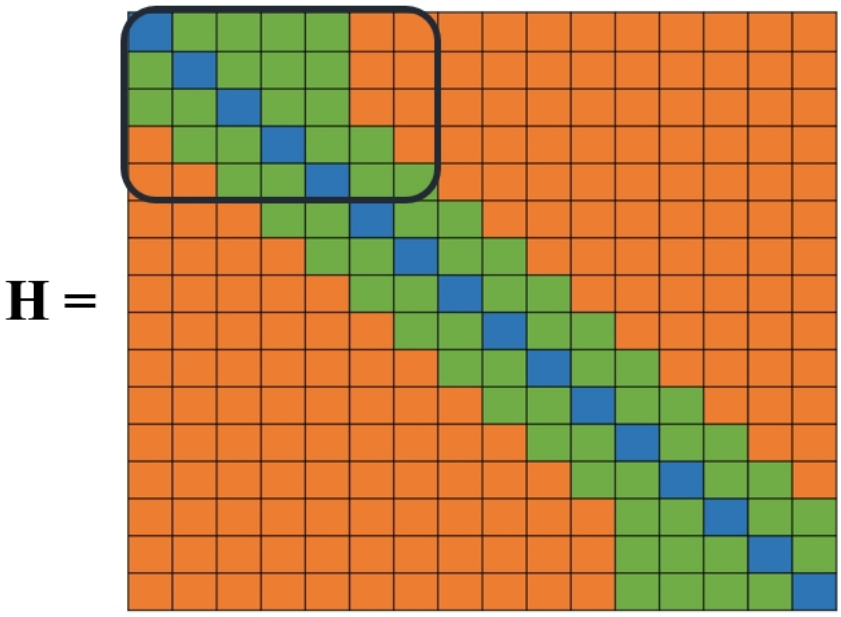

FIG. F29: The structure of Hamiltonian matrix in small size representation. The coefficient occupy five columns (show in green and blue), the non-derivative term like $k(x)$ are present in diagonal (showed in blue), and other term is zero (showed in orange).

(C_0/h^2) $+ \mathrm{k}(x_0)$	(C_1/h^2)	(C_2/h^2)	(C_3/h^2)	(C_4/h^2)	0	0
(C_0/h^2)	(C_1/h^2) $+ \mathrm{k}(x_1)$	(C_2/h^2)	(C_3/h^2)	(C_4/h^2)	0	0
(C_0/h^2)	(C_1/h^2)	(C_2/h^2) $+ \mathrm{k}(x_2)$	(C_3/h^2)	(C_4/h^2)	0	0
0	(C_0/h^2)	(C_1/h^2)	(C_2/h^2) $+ \mathrm{k}(x_3)$	(C_3/h^2)	(C_4/h^2)	0
0	0	(C_0/h^2)	(C_1/h^2)	(C_2/h^2) $+ \mathrm{k}(x_4)$	(C_3/h^2)	(C_4/h^2)

FIG. F30: Zoom up of the marked region of the H-matrix shown in Fig. F29.

The structure of Hamiltonian matrices (**H**) is defined in Fig. F29 and zoom up of marked region is shown in Fig. F30. To obtain all eigenvalues(ro-vibrational energies) as real numbers, the first and last two columns and the first and last two rows of **H** are removed, and then **H** become a square matrix. Diagonalization of the Hamiltonian matrix, gives us a square matrix consisting of eigenvalues as the diagonals, and a square matrix consisting of eigenvectors.

B. Implementation

We have implemented the procedure for the solution of the 1-D Schroedinger equation (Eqn. E25) using the described methodology in a Python program. We utilize the NumPy[53, 55, 59] module for this purpose. In our implementation, we have the freedom to choose the step (h), stencil number (or order of the derivative expansion), the user-provided potential curve and the atomic masses.

Eigen-decomposition of the H-matrix is performed using `linalg` module of NumPy. The function returns the eigenvalues and eigen-vectors, corresponding to the the ro-vibrational states. Normalization of the eigen-

vectors is performed at a later stage.

C. Result

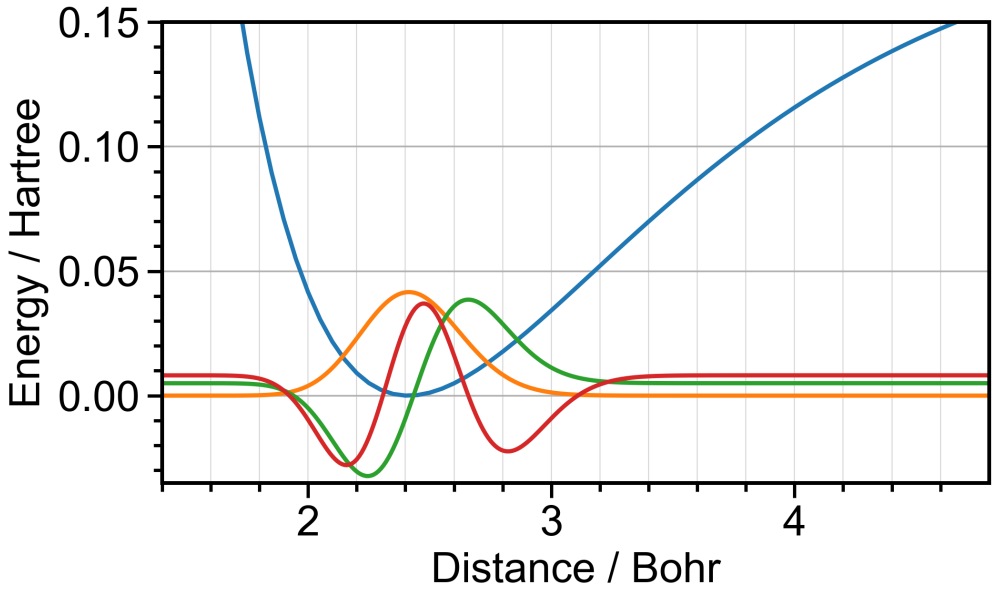

FIG. F31: Potential energy curve of HCl molecule with the obtained ro-vibrational wavefunctions for the $v = 0 - 3$, $J = 0$ states using the collocation method.

S6. Additional details on the coupled-cluster calculations

In order to check the multireference character of the coupled-cluster electronic wave functions, the T1 and T2 amplitudes across the internuclear distance were analyzed. These are plotted in Fig. F32 and F33. These plots suggest that the shortcomings in the computed CCSD(T) polarizabilities are associated with the inappropriateness of the single-reference CC ansatz for stretched molecules. The presented results suggest that the multireference character of the studied wave functions becomes important already for the distances associated with vibrational displacements of the studied here molecules. This multireference character has quite large impact on the computed polarizabilities, but surprisingly, it does not affect much the portions of the CCSD(T) potential energy surfaces in the vibrational region, as visible in Fig. 4 of the manuscript.

A comparison of the CCSD(T) potential energy curves with the "experimental anharmonic potential energy curves" obtained by fitting vibrational molecular energy levels and transition energies is given in Fig. F34. The deviations between the CCSD(T) PES and the accurate anharmonic PES appear for all the molecules at larger internuclear distances, but it does not seem to affect the region associated with the fundamental vibration. Notable discontinuity is observed for the CO molecule at 4 bohr which corresponds to the discontinuity seen for the polarizability components (see Fig. 4 in the manuscript) and is most likely associated with the sudden change in the wave function character.

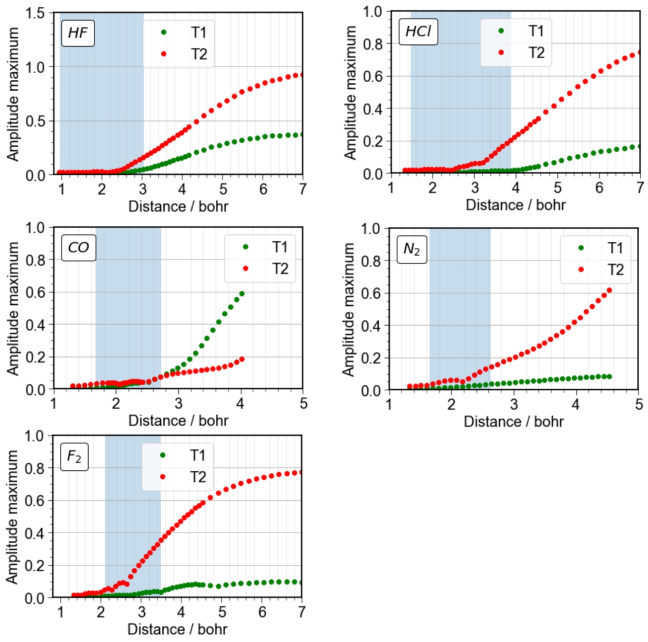

FIG. F32: Maximum of the T1 and T2 amplitudes encountered during the CCSD(T) calculations for five studied molecules in this work. The following figure (Fig. F33) shows the zoomed up region of the same data.

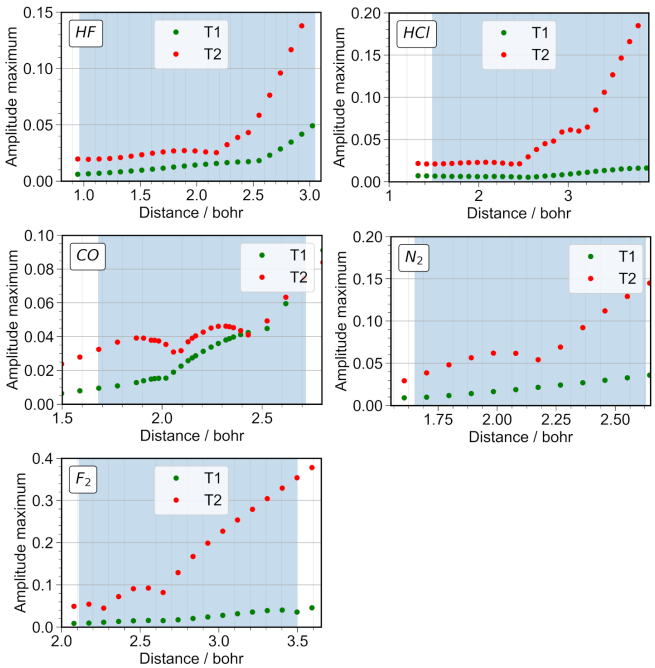

FIG. F33: Maximum of the T1 and T2 amplitudes encountered during the CCSD(T) calculations for five studied molecules in the region spanned by the ground and first vibrational wave functions (region marked in blue color). The y-scale was scaled in order to focus on the T1 amplitudes.

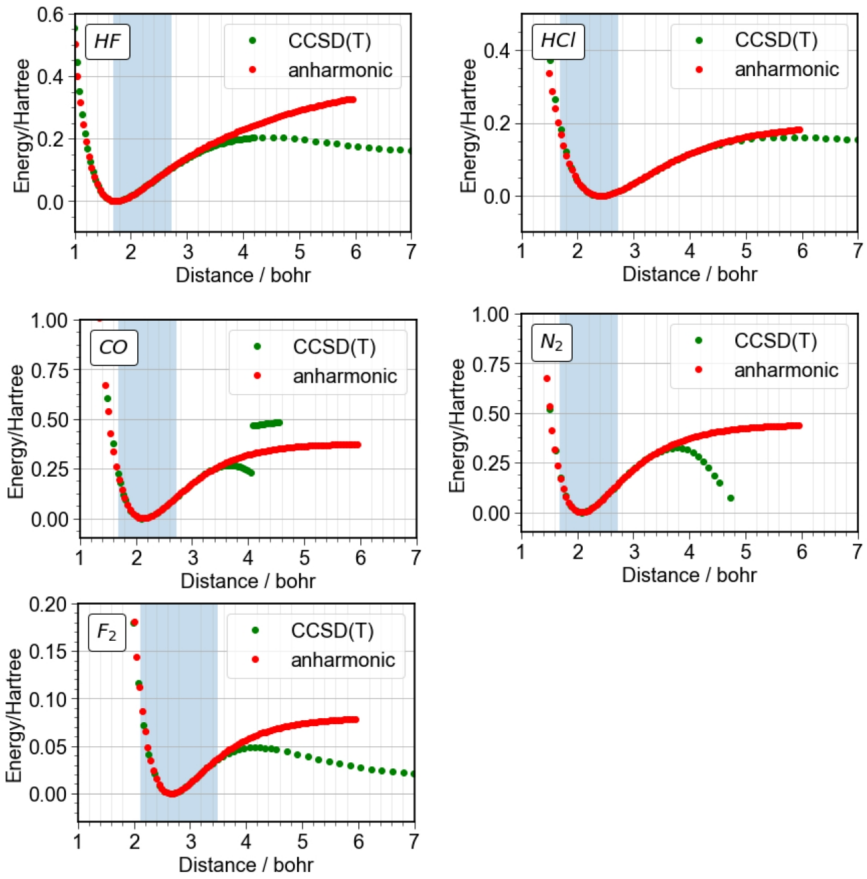

FIG. F34: Comparison of the coupled-cluster potential energy curve (in green) with the corresponding anharmonic potential energy curve (in red) obtained from our analysis of experimental transition frequencies. The CCSD(T) energies were re-scaled to zero in order to plot the two curves together.

Bibliography

[1] I. Gordon, L. Rothman, R. Hargreaves, R. Hashemi, E. Karlovets, F. Skinner, E. Conway, C. Hill, R. Kochanov, Y. Tan, P. Wcisło, A. Finenko, K. Nelson, P. Bernath, M. Birk, V. Boudon, A. Campargue, K. Chance, A. Coustenis, B. Drouin, J. Flaud, R. Gamache, J. Hodges, D. Jacquemart, E. Mlawer, A. Nikitin, V. Perevalov, M. Rotger, J. Tennyson, G. Toon, H. Tran, V. Tyuterev, E. Adkins, A. Baker, A. Barbe, E. Canè, A. Császár, A. Dudaryonok, O. Egorov, A. Fleisher, H. Fleurbaey, A. Foltynowicz, T. Furtenbacher, J. Harrison, J. Hartmann, V. Horneman, X. Huang, T. Karman, J. Karns, S. Kassi, I. Kleiner, V. Kofman, F. Kwabia–Tchana, N. Lavrentieva, T. Lee, D. Long, A. Lukashevskaya, O. Lyulin, V. Makhnev, W. Matt, S. Massie, M. Melosso, S. Mikhailenko, D. Mondelain, H. Müller, O. Naumenko, A. Perrin, O. Polyansky, E. Raddaoui, P. Raston, Z. Reed, M. Rey, C. Richard, R. Tóbiás, I. Sadiek, D. Schwenke, E. Starikova, K. Sung, F. Tamassia, S. Tashkun, J. V. Auwera, I. Vasilenko, A. Vigasin, G. Villanueva, B. Vispoel, G. Wagner, A. Yachmenev, and S. Yurchenko, The HITRAN2020 molecular spectroscopic database, Journal of Quantitative Spectroscopy and Radiative Transfer **277**, 107949 (2022).

[2] A. Pine and J. Looney, N_2 and air broadening in the fundamental bands of HF andHCl, Journal of Molecular Spectroscopy **122**, 41 (1987).

[3] G. Guelachvili and M. Smith, Measurements of pressure-induced shifts in the 1-0 and 2-0 bands of HF and in the 2-0 bands of $H^{35}Cl$ and $H^{37}Cl$, Journal of Quantitative Spectroscopy and Radiative Transfer **20**, 35 (1978).

[4] A. Pine and A. Fried, Self-broadening in the fundamental bands of HF and HCl, Journal of Molecular Spectroscopy **114**, 148 (1985).

[5] R. Meredith and F. Smith, Broadening of hydrogen fluoride lines by H_2, D_2, and N_2, Journal of Chemical Physics **60**, 3388 (1974).

[6] R. Meredith, Strengths and widths in the first overtone band of hydrogen fluoride, Journal of Quantitative Spectroscopy and Radiative Transfer **12**, 485 (1972).

[7] S.-I. Chou, D. Baer, and R. Hanson, Spectral intensity and lineshape measurements in the first overtone band of HF using tunable diode lasers, Journal of Molecular Spectroscopy **195**, 123 (1999).

[8] K. Chance, K. Jucks, D. Johnson, and W. Traub, The Smithsonian astrophysical observatory database SAO92, Journal of Quantitative Spectroscopy and Radiative Transfer **52**, 447 (1994).

[9] G. Bachet, Etude sur les elargissements par des gaz etrangers comprimés des raies du spectre de rotation pure de la molécule HF-II. perturbation par les molécules linéaires homopolaires, Journal of Quantitative Spectroscopy and Radiative Transfer **14**, 1285 (1974).

[10] J. Coxon and P. Hajigeorgiou, Breakdown of the Born-Oppenheimer approximation in the ground electronic state of hydrogen halides: improved direct potential fitting analyses for HF/DF/TF. HCl/DCl/TCl, HBr/DBr/TBr and HI/DI/TI, Journal of Quantitative Spectroscopy and Radiative Transfer **151**, 133 (2015).

[11] S.-I. Chou, D. Baer, and R. Hanson, Diode–laser measurements of He-, Ar-, and N_2-broadened HF lineshapes in the first overtone band, Journal of Molecular Spectroscopy **196**, 70 (1999).

[12] G. Li, I. Gordon, R. L. Roy, P. Hajigeorgiou, J. Coxon, P. Bernath, and L. Rothman, Reference spectroscopic data for hydrogen halides. Part I: Construction and validation of the ro-vibrational dipole moment functions, Journal of Quantitative Spectroscopy and Radiative Transfer **121**, 78 (2013).

[13] J. Ogilvie and Y.-P. Lee, Line strengths in the 3-0 vibration-rotational band of gaseous $^1H^{35}Cl$ and electric dipole moment function, Chemical Physics Letters **159**, 239 (1989).

[14] K. Park, K. Chance, I. Nolt, J. Radostitz, and M. Vanek, Pressure broadening of the 2.5 THz $H^{35}Cl$ rotational line by N_2 and O_2, Journal of Molecular Spectroscopy **147**, 521 (1991).

[15] M. D. Rosa, C. Nardini, C. Piccolo, C. Corsi, and F. D'Amato, Pressure broadening and shift of transitions of the first overtone of HCl, Applied Physics B: Lasers and Optics **72**, 245 (2001).

[16] B. Drouin, Temperature dependent pressure-induced lineshape of the HCl $J = 1 \leftarrow 0$ rotational transition in nitrogen and oxygen, Journal of Quantitative Spectroscopy and Radiative Transfer **83**, 321 (2004).

[17] I. Morino and K. Yamada, Absorption profiles of HCl for the J=1–0 rotational transition: Foreign-gas effects measured for N_2, O_2, and Ar, Journal of Molecular Spectroscopy **233**, 77 (2005).

[18] M. Zughul, J. Gelfand, H, Rabitz, and A. E. DePristo, Pressure broadening in the 0-4 through 0-7 overtone bands of $H^{35}Cl$ and $H^{37}Cl$, Journal of Quantitative Spectroscopy and Radiative Transfer **24**, 371 (1980).

[19] G. Cazzoli and C. Puzzarini, Hyperfine structure of the J= $1 \leftarrow 0$ transition of $H^{35}Cl$ and $H^{37}Cl$: improved ground state parameters, Journal of Molecular Spectroscopy **226**, 161 (2004).

[20] J. A. Coxon, P. G. Hajigeorgiou, and R. J. L. Roy, Improved direct potential fit analyses for the ground electronic states of the hydrogen halides: HF/DF/TF, HCl /DCl /TCl, HBr/DBr/TBr and HI/DI/TI, Journal of Quantitative Spectroscopy and Radiative Transfer **151**, 133 (2015).

[21] G. Li, I. Gordon, P. Bernath, and L. Rothman, Direct fit of experimental ro-vibrational intensities to the dipole moment function: Application to HCl, Journal of Quantitative Spectroscopy and Radiative Transfer **112**, 1543 (2011).

[22] M. Tudorie, T. Földes, A. Vandaele, and J. V. Auwera, CO_2 pressure broadening and shift coefficients for the 1-0 band of HCl and DCl, Journal of Quantitative Spectroscopy and Radiative Transfer **113**, 1092 (2012).

[23] C. Crane-Robinson and H. Thompson, Pressure broadening studies on vibration-rotation bands. IV. Optical collision diameters for foreign-gas broadening of CO and DCl bands, Proceedings of the Royal Society A **272**, 453 (1963).

[24] G. Cazzoli and C. Puzzarini, Hyperfine structure of the J = $1 \leftarrow 0$ and J = $2 \leftarrow 1$ transitions of $D^{35}Cl$ and $D^{37}Cl$, Physical Chemistry Chemical Physics **6**, 5133 (2004).

[25] C. Pollock, F. Petersen, D. Jennings, and J. Wells, Absolute frequency measurements of the 2-0 band of CO at 2.3 μm;

calibration standard frequencies from high resolution color center laser spectroscopy, Journal of Molecular Spectroscopy **99**, 357 (1983).
[26] Q. Zou and P. Varanasi, New laboratory data on the spectral line parameters in the 1-0 and 2-0 bands of $^{12}C^{16}O$ relevant to atmospheric remote sensing, Journal of Quantitative Spectroscopy and Radiative Transfer **75**, 63 (2002).
[27] K. Sung and P. Varanasi, Intensities, collision-broadened half-widths, and collision-induced line shifts in the second overtone band of $^{12}C^{16}O$, Journal of Quantitative Spectroscopy and Radiative Transfer **83**, 445 (2004).
[28] J. A. Coxon and P. Hajigeorgiou, Direct potential fit analysis of the $X^1\Sigma^+$ ground state of CO, Journal of Chemical Physics **121**, 2992 (2004).
[29] V. M. Devi, D. C. Benner, M. A. H. Smith, A. Mantz, K. Sung, L. R. Brown, and A. Predoi-Cross, Spectral line parameters including temperature dependences of self- and air-broadening in the 2 $\rightarrow$ 0 band of CO at 2.3 μm, Journal of Quantitative Spectroscopy and Radiative Transfer **113**, 1013 (2012).
[30] V. M. Devi, D. C. Benner, M. A. H. Smith, A. Mantz, K. Sung, L. R. Brown, and A. Predoi-Cross, Erratum to "Spectral line parameters including temperature dependences of self- and air-broadening in the 2 $\rightarrow$ 0 band of CO at 2.3 μm ", Journal of Quantitative Spectroscopy and Radiative Transfer **116**, 199 (2013).
[31] G. Li, I. Gordon, L. Rothman, Y. Tan, S.-M. Hu, S. Kassi, A. Campargue, and E. Medvedev, Rovibrational line lists for nine isotopologues of the CO molecule in the $X^1\Sigma^+$ ground electronic state, The Astrophysical Journal Supplement Series **216**, 15 (2015).
[32] V. M. Devi, D. C. Benner, K. Sung, T. J. Crawford, G. Li, R. R. Gamache, M. A. H. Smith, I. E. Gordon, and A. W. Mantz, Positions, intensities and line shape parameters for the 1$\leftarrow$0 bands of CO isotopologues, Journal of Quantitative Spectroscopy and Radiative Transfer **218**, 203 (2018).
[33] D. Mondelain, T. Sala, S. Kassi, D. Romanini, M. Marangoni, and A. Campargue, Broadband and highly sensitive comb-assisted cavity ring down spectroscopy of CO near 1.57 μm with sub-MHz frequency accuracy, Journal of Quantitative Spectroscopy and Radiative Transfer **154**, 35 (2015).
[34] A. Cygan, P. Wcisło, S. Wójtewicz, G. Kowzan, M. Zaborowski, D. Charczun, K. Bielska, R. S. Trawiński, R. Ciuryło, P. Masłowski, and D. Lisak, High-accuracy and wide dynamic range frequency-based dispersion spectroscopy in an optical cavity, Optics Express **27**, 21810 (2019).
[35] Y. Borkov, A. Solodov, A. Solodov, T. Petrova, E. Karlovets, and V. Perevalov, Fourier transform CO spectra near 1.6 μm, Journal of Quantitative Spectroscopy and Radiative Transfer **253**, 107064 (2020).
[36] R. Hashemi, I. E. Gordon, E. M.Adkins, J. T. Hodges, D. A. Long, M. Birk, J. Loos, C. D.Boone, A. Fleisher, A. Predoi-Cross, and L. S. Rothman, Improvement of the spectroscopic parameters of the air- and self-broadened N_2O and CO lines for the HITRAN2020 database applications, Journal of Quantitative Spectroscopy and Radiative Transfer **271**, 107735 (2021).
[37] S. Tashkun, T. Velichko, and S. Mikhailenko, Critical evaluation of measured pure-rotation and rotation-vibration line positions and an experimental dataset of energy levels of $^{12}C^{16}O$ in $X^1\Sigma^+$ state, Journal of Quantitative Spectroscopy and Radiative Transfer **111**, 1106 (2010).
[38] V. M. Devi, D. C. Benner, M. A. H. Smith, A. Mantz, K. Sung, and L. R. Brown, Spectral line parameters including temperature dependences of air-broadening for the 2 $\rightarrow$ 0 bands of $^{13}C^{16}O$ and $^{12}C^{18}O$ at 2.3 μm, Journal of Molecular Spectroscopy **276-277**, 33 (2012).
[39] R. L. Roy, Y. Huang, and C. Jary, An accurate analytic potential function for ground-state N_2 from a direct-potential-fit analysis of spectroscopic data, Journal of Chemical Physics **125**, 164310 (2006).
[40] H. Li and R. L. Roy, Quadrupole moment function and absolute infrared quadrupolar intensities for N_2, Journal of Chemical Physics **126**, 22 (2007).
[41] A. Goldman, R. Tipping, Q. Ma, C. Boone, P. Bernath, P. Demoulin, F. Hase, M. Schneider, J. Hannigan, M. Coffey, and C. Rinsland, On the line parameters for the $X^1\Sigma_g^+$ (1-0) infrared quadrupolar transitions of $^{14}N_2$, Journal of Quantitative Spectroscopy and Radiative Transfer **103**, 168 (2007).
[42] H. G. M. Edwards, E. A. M. Good, and D. A. Long, Pure rotational Raman spectrum of fluorine, J. Chem. Soc., Faraday Trans. 2 **72**, 984 (1976).
[43] R. Martinez, D. Bermejo, J. Santos, and P. Cancio, High-resolution stimulated Raman spectrum of F_2, Journal of Molecular Spectroscopy **168**, 343 (1994).
[44] L. Bytautas and K. Ruedenberg, Ab initio potential energy curve of F_2. IV. Transition from the covalent to the van der Waals region: Competition between multipolar and correlation forces, The Journal of Chemical Physics **130**, 204101 (2009).
[45] A. Raj, H. Hamaguchi, and H. A. Witek, Polarizability tensor invariants of H_2 , HD and D_2, J. Chem. Phys. **148**, 104308 (2018).
[46] J. Rychlewski, A Variation-Perturbation calculation of the dynamic polarizability of the H_2 molecule, Chem. Phys. Lett. **73**, 135 (1980).
[47] B. P. Pritchard, D. Altarawy, B. Didier, T. D. Gibson, and T. L. Windus, New basis set exchange: An open, up-to-date resource for the molecular sciences community, Journal of Chemical Information and Modeling **59**, 4814 (2019).
[48] P. M. Morse, Diatomic molecules according to the wave mechanics. II. vibrational levels, Physical Review **34**, 57 (1929).
[49] Y. P. Varshni, Comparative study of potential energy functions for diatomic molecules, Reviews of Modern Physics **29**, 664 (1957).
[50] R. Rydberg, Graphische darstellung einiger bandenspektroskopischer ergebnisse, Zeitschrift für Physik **73**, 376 (1932).
[51] H. Y. Abdullah, A comparative study of potential energy curves with RKRV curves for the ground states of i2, f2

and CO molecules, Bulletin of Materials Science **42**, 10.1007/s12034-019-1824-2 (2019).
[52] J. P. Araújo and M. Y. Ballester, A comparative review of 50 analytical representation of potential energy interaction for diatomic systems: 100 years of history, International Journal of Quantum Chemistry **121**, 10.1002/qua.26808 (2021).
[53] E. Jones, T. Oliphant, P. Peterson, *et al.*, SciPy: Open source scientific tools for Python (2001–), accessed: 2019-01-25.
[54] P. Virtanen, R. Gommers, T. E. Oliphant, M. Haberland, T. Reddy, D. Cournapeau, E. Burovski, P. Peterson, W. Weckesser, J. Bright, S. J. van der Walt, M. Brett, J. Wilson, K. J. Millman, N. Mayorov, A. R. J. Nelson, E. Jones, R. Kern, E. Larson, C. J. Carey, İ. Polat, Y. Feng, E. W. Moore, J. VanderPlas, D. Laxalde, J. Perktold, R. Cimrman, I. Henriksen, E. A. Quintero, C. R. Harris, A. M. Archibald, A. H. Ribeiro, F. Pedregosa, P. van Mulbregt, A. Vijaykumar, A. P. Bardelli, A. Rothberg, A. Hilboll, A. Kloeckner, A. Scopatz, A. Lee, A. Rokem, C. N. Woods, C. Fulton, C. Masson, C. Häggström, C. Fitzgerald, D. A. Nicholson, D. R. Hagen, D. V. Pasechnik, E. Olivetti, E. Martin, E. Wieser, F. Silva, F. Lenders, F. Wilhelm, G. Young, G. A. Price, G.-L. Ingold, G. E. Allen, G. R. Lee, H. Audren, I. Probst, J. P. Dietrich, J. Silterra, J. T. Webber, J. Slavič, J. Nothman, J. Buchner, J. Kulick, J. L. Schönberger, J. V. de Miranda Cardoso, J. Reimer, J. Harrington, J. L. C. Rodríguez, J. Nunez-Iglesias, J. Kuczynski, K. Tritz, M. Thoma, M. Newville, M. Kümmerer, M. Bolingbroke, M. Tartre, M. Pak, N. J. Smith, N. Nowaczyk, N. Shebanov, O. Pavlyk, P. A. Brodtkorb, P. Lee, R. T. McGibbon, R. Feldbauer, S. Lewis, S. Tygier, S. Sievert, S. Vigna, S. Peterson, S. More, T. Pudlik, T. Oshima, T. J. Pingel, T. P. Robitaille, T. Spura, T. R. Jones, T. Cera, T. Leslie, T. Zito, T. Krauss, U. Upadhyay, Y. O. Halchenko, and Y. V.-B. and, SciPy 1.0: fundamental algorithms for scientific computing in python, Nature Methods **17**, 261 (2020).
[55] F. Gao and L. Han, Implementing the Nelder-Mead simplex algorithm with adaptive parameters, Computational Optimization and Applications **51**, 259 (2010).
[56] K. P. Huber and G. Herzberg, Constants of diatomic molecules, in *Molecular Spectra and Molecular Structure: IV. Constants of Diatomic Molecules* (Springer US, Boston, MA, 1979) pp. 8–689.
[57] T. Todd, C. Clayton, W. Telfair, T. McCubbin, and J. Plíva, Infrared emission of 12c16o, 13c16o, and 12c18o, Journal of Molecular Spectroscopy **62**, 201 (1976).
[58] T. R. Gilson, I. R. Beattie, J. D. Black, D. A. Greenhalgh, and S. N. Jenny, Redetermination of some of the spectroscopic constants of the electronic ground state of di-nitrogen 14n2, 14n15n and 15n2 using coherent anti-stokes raman spectroscopy, Journal of Raman Spectroscopy **9**, 361 (1980).
[59] C. R. Harris, K. J. Millman, S. J. van der Walt, R. Gommers, P. Virtanen, D. Cournapeau, E. Wieser, J. Taylor, S. Berg, N. J. Smith, R. Kern, M. Picus, S. Hoyer, M. H. van Kerkwijk, M. Brett, A. Haldane, J. F. del Río, M. Wiebe, P. Peterson, P. Gérard-Marchant, K. Sheppard, T. Reddy, W. Weckesser, H. Abbasi, C. Gohlke, and T. E. Oliphant, Array programming with NumPy, Nature **585**, 357 (2020).